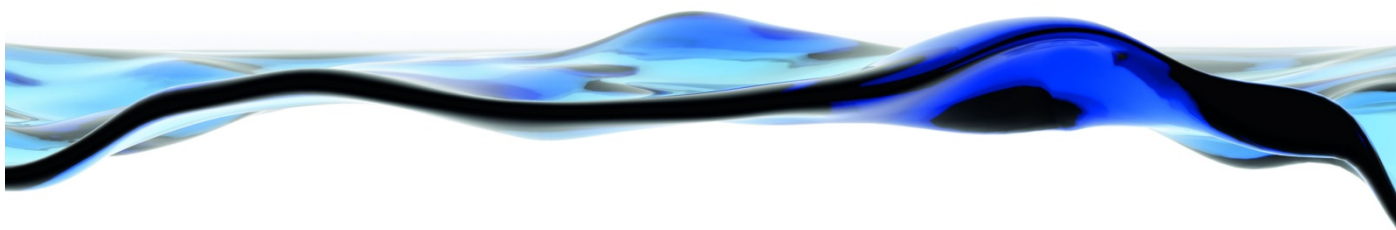


Assessment of Adelaide Plains Groundwater Resources: Summary Report



Goyder Institute for Water Research
Technical Report Series No. 15/31



www.goyderinstitute.org

Goyder Institute for Water Research Technical Report Series ISSN: 1839-2725

The Goyder Institute for Water Research is a partnership between the South Australian Government through the Department of Environment, Water and Natural Resources, CSIRO, Flinders University, the University of Adelaide and the University of South Australia. The Institute will enhance the South Australian Government's capacity to develop and deliver science-based policy solutions in water management. It brings together the best scientists and researchers across Australia to provide expert and independent scientific advice to inform good government water policy and identify future threats and opportunities to water security.



Government
of South Australia

Department of Environment,
Water and Natural Resources



THE UNIVERSITY
of ADELAIDE



University of
South Australia



Flinders
UNIVERSITY
ADELAIDE • AUSTRALIA

The following associate organisation contributed to the report:



Enquires should be addressed to: Goyder Institute for Water Research
Level 4, 33 King William Street
Adelaide, SA, 5000
tel: 08-8236 5200
e-mail: enquiries@goyderinstitute.org

Citation

Bresciani E, Batelaan O, Banks EW, Barnett SR, Batlle-Aguilar J, Cook PG, Costar A, Cranswick RH, Doherty J, Green G, Kozuskanich J, Partington D, Pool M, Post VEA, Simmons CT, Smerdon BD, Smith SD, Turnadge C, Villeneuve S, Werner AD, White N and Xie Y, 2015, *Assessment of Adelaide Plains Groundwater Resources: Summary Report*, Goyder Institute for Water Research Technical Report Series No. 15/31, Adelaide, South Australia

Copyright

© 2015 Flinders University. To the extent permitted by law, all rights are reserved and no part of this publication covered by copyright may be reproduced or copied in any form or by any means except with the written permission of Flinders University.

Disclaimer

The Participants advise that the information contained in this publication comprises general statements based on scientific research and does not warrant or represent the completeness of any information or material in this publication.

Foreword

This document presents a summary of the outcomes of the Goyder Institute for Water Resources project I.1.6 'The assessment of the Adelaide Plains groundwater resources' conducted by a team of researchers of Flinders University and CSIRO during the project period 15 May 2013 – 31 May 2015 in close collaboration with the Department of Environment Water and Natural Resources (DEWNR).

Contents

Foreword	i
Acknowledgments	viii
Executive summary.....	ix
1 Introduction	1
Part I Field and Desktop Investigations	3
2 Hydrogeological setting.....	4
2.1 Geology	4
2.2 Hydrostratigraphy	4
2.3 Aquifer and aquitard properties	10
2.4 Groundwater salinity	11
2.5 Groundwater potentiometric surfaces	15
2.6 Groundwater use	18
3 Diffuse groundwater recharge	20
3.1 Introduction	20
3.2 Chloride mass balance approach	20
4 Groundwater-surface water interaction	21
4.1 Introduction	21
4.2 Differential stream gauging approach	21
5 Flow across the faults.....	23
5.1 Introduction	23
5.2 Geochemical analysis.....	24
5.3 Comparison to the Willunga Embayment.....	25
6 Leakage through the Munno Para Clay.....	27
6.1 Introduction	27
6.2 Vertical hydraulic conductivity and leakage estimates	27
Part II Regional Groundwater Modelling	29
7 Model setup and calibration	30
7.1 Model extent and hydrostratigraphy.....	30
7.2 Flow models (historical).....	32
7.3 Flow models (future).....	35
7.4 Calibration.....	35
8 Water balance and its evolution	37
8.1 Pre-development (before 1950)	37
8.2 Development to present (1950–2013)	39
8.3 Future (2013–2100)	41

9	Model capabilities and limitations	44
Part III Synthesis		45
10	Comparison of approaches and ways forward	46
	10.1 Diffuse groundwater recharge.....	46
	10.2 Groundwater-surface water interaction.....	46
	10.3 Flow across the faults	47
	10.4 Leakage through the Munno Para Clay.....	47
11	Revised groundwater flow mechanisms	48
12	Implications for groundwater resources management	51
13	Recommendations	52
14	References.....	53

Figures

Figure 1 Generalised geology showing the Northern and Central Adelaide Plains, Western Mount Lofty Ranges and the numerical groundwater model boundary	5
Figure 2 Generalised hydrogeology showing the Quaternary, T1, T2 and Fractured Rock aquifer extents in addition to the currently operational State Observation Bore Network. Note that the indicated northern bounds of the Quaternary and T2 aquifers are the boundaries of the Prescribed Wells Area; the aquifers do in fact extend further north	6
Figure 3 Cross-sections through the Central Adelaide Plains and the Golden Grove Embayment (Gerges 1999).....	8
Figure 4 Three-dimensional visualisation of the hydrostratigraphic units used in the numerical groundwater model (vertical exaggeration x10). One or several units are removed (starting from the shallowest) from Figure (a) through to Figure (g), making the deeper units visible.....	9
Figure 5 Most recent groundwater salinity (expressed in units of electrical conductivity EC) for Quaternary aquifers (and additionally bores whose maximum drilled depth was between 0 m and 30 m) and Fractured Rock aquifers at any depth	12
Figure 6 Most recent groundwater salinity (expressed in units of electrical conductivity EC) for T1 and T2 aquifers shows broad corridors of good quality groundwater in much of the study area in both aquifers....	13
Figure 7 Graphs showing (left) the ratio of Cl / (TIC + SO ₄) versus the chloride concentration and (right) the ratio of Na / (K + Ca + Mg) versus the chloride concentration. Ratios are based on concentrations expressed in meq L ⁻¹ . Numbered lines represent the relationships resulting from mixing between freshwater and seawater (1), freshwater and hypersaline water (2) and seawater and hypersaline water (3). Black lines are based on the most saline sample from the Willunga area (WLG096), grey lines are based on the most saline sample from the Adelaide Plains area (YAT067). Coloured symbols except cyan stars represent samples from the Willunga Embayment (see appendix G for details), grey symbols are data points for the Adelaide Plains area obtained from the WaterConnect database. Cyan stars represent samples obtained in the new observation wells drilled for this study (Appendix E)	13
Figure 8 Locations of saline groundwater across the Adelaide Plains with size and shape indicating salinity (mg L ⁻¹). Marker symbol indicate if sample has a hydrochemical signature of hypersaline water (triangles) or unknown (circles). The samples span different aquifers but are mostly from the T3, T4 and FRA aquifers, and were taken between 1966 and 2005	14
Figure 9 Potentiometric surfaces for the T1 aquifer in March 2014 (courtesy of DEWNR).....	16
Figure 10 Potentiometric surfaces for the T2 aquifer in March 2014 (courtesy of DEWNR).....	17
Figure 11 Current licensed groundwater allocation for all aquifers in the NAP and CAP in addition to MAR scheme location and status.....	19
Figure 12 Groundwater – surface water exchange rates for Brownhill creek at four separate gauging times show generally consistent trends of losing conditions below the fault and gaining conditions above the fault. Temporal variability in exchange flux is thought to be due to the changing hydraulic head gradients between the creek and underlying/adjacent aquifers in time. Black circles indicate gauging locations and creek flow direction is from southeast to northwest	22
Figure 13 Conceptual model of groundwater flow and groundwater – surface water exchange in the vicinity of Brownhill Creek.....	22
Figure 14 Conceptual model of flow across the Eden-Burnside Fault (after Green <i>et al.</i> 2010)	23
Figure 15 Hydrograph comparison for Fractured Rock aquifer monitoring bores east and west of the Eden Burnside fault along 5 th creek. The horizontal distances between ADE133 east of the fault and ADE147 and ADE168 west of the fault are 353 and 697 m respectively.	24

Figure 16 Carbon-14 ages along the North, Central and South Transects (top, middle and bottom respectively) show increasing age towards the coast (0 km) for the T1 and T2 aquifers with dashed lines indicating the location of faults.....	25
Figure 17 Site 13 modelled helium concentrations for (a) Scenario 1 and (b) Scenario 3 – further discussed in Appendix F.....	28
Figure 18 Year 2014 hydraulic head difference map between the T2 and T1 aquifers (units of metres), constructed using different sources and a Bayesian Data Fusion approach (details given in Appendix F). A negative difference implies downward leakage and positive difference implies upwards leakage	28
Figure 19 (a) Regional setting indicating the model extent and (b) selected cross-sections revealing the hydrostratigraphy as implemented in the model. The shorthand names for the zones are defined in Table 3	31
Figure 20 Conductance of the eastern GHB cells (3D view) when K equals the preferred value in all units. The distribution of values reflects differences in the area connecting the cells to the external source (product of the cell thickness by the length of boundary line crossing the cell)	32
Figure 21 Conceptualization of the coastal boundary.....	33
Figure 22 (a) All surface water features, considered in the winter months, and (b) perennial surface water features, considered in the summer months.....	33
Figure 23 (a) Average annual rainfall distribution (1889–2013) and (b) location of pumping wells	34
Figure 24 Monthly net pumping rates applied to the entire model domain, T1 and T2 aquifers	34
Figure 25 (a) Vertical flux through T1 top, and (b) groundwater-surface water exchange rates, both for the steady-state historical flow model.....	38
Figure 26 Monthly water balance for the transient development to present model (1950–2013) for the whole model and for the individual T1 and T2 aquifers. For clarity, only the units exchanging significantly with the T1 and T2 aquifers are shown.....	40
Figure 27 Yearly water balance for the transient development to present model (1950–2013) for the whole model and for the individual T1 and T2 aquifers. For clarity, only the units exchanging significantly with the T1 and T2 aquifers are shown.....	40
Figure 28 Cumulative change in storage (GL) for the development to present model (1950–2013) for units showing a significant storage change.....	41
Figure 29 Cumulative changes in storage (GL) for the base case scenario (2013–2100) for units showing a significant storage change.....	42
Figure 30 Comparison of cumulative storage change between base case, increased pumping, decreased pumping and increased MAR future scenarios (after the vertical dashed line which indicates the start of the year 2013) for units showing a significant storage change.....	43
Figure 31 Decadal average water balance components as a percentage of the total balance for pre-development (in 1950), development (in 2012) and future (base-case in 2050) periods. Red coloured pieces of the pie indicate flow out of the system, blue pieces indicate flow into the system, and green indicates storage changes (either gain or loss)	49
Figure 32 Hydrogeological conceptual model of the Adelaide Plains groundwater resources	50

Tables

Table 1 Stratigraphy and hydrostratigraphy of the Adelaide Plains (Zulfic <i>et al.</i> 2008)	7
Table 2 Summary of vertical hydraulic conductivity (K_v), horizontal hydraulic conductivity (K_h) and specific storage (S_s) values determined from hydraulic tests on core samples or from in-situ pumping (after Gerges (1999), Gerges (2006) and Hodgkin (2004) in addition to values derived in this study). Q stands for Quaternary, T for Tertiary	10
Table 3 Hydrostratigraphic units (zones of constant properties) and their abbreviation.....	31
Table 4 Summary of different scenarios applied including climate change, increased groundwater pumping and increased managed aquifer recharge	35
Table 5 Model performance statistics (definitions and keys for interpretation are given in Apx Table K.4) ..	36
Table 6 Decadal average annual fluxes (GL yr^{-1}) at the end of the transient pre-development model (1939–1949). Fluxes are from zones or boundaries indicated by the row names to other zones or boundaries indicated by the column names (except for the last row which indicates the change in storage in zones indicated by the column names). Values below 1×10^{-2} are not shown. Colours are indicative of the magnitude, with blue to red colours highlighting small to large fluxes respectively as indicated in the lower table	38
Table 7 Decadal average annual fluxes (GL yr^{-1}) at the end of the transient development model (2002–2012). Reading keys are given in the caption of Table 6.....	41
Table 8 Decadal average annual fluxes (GL yr^{-1}) during the base case future model (2040–2050). Reading keys are given in the caption of Table 6.....	42
Table 9 Difference between base case and RCP4.5 scenarios in the decadal (2040–2050) average annual flux matrix (GL yr^{-1}). Values below 1×10^{-2} are not shown.....	43

Acknowledgments

Funding for this project was provided through joint funding between the Goyder Institute for Water Research, CSIRO, Flinders University, NCGRT and DEWNR. Investigations in the Willunga catchment were also supported by funding from the National Collaborative Research Infrastructure Scheme. Field work including drilling supervision and groundwater and creek sampling was completed by the authors in addition to Nicholas Kruger, Jordi Batlle-Aguilar, Nicholas White, Lawrence Burke and Robert Andrew. Brian Smerdon designed the vibrating wire project and helped with the initial scoping of the study. Adrian Costar and Eddie Banks helped with the installation of the vibrating wires and Stacey Priestley helped with core collection at Site 13. We also wish to thank Glenn Harrington and a CSIRO reviewer for their constructive comments on earlier drafts of this report.

Executive summary

This project investigated the groundwater resources of the Adelaide Plains with the aims to (i) improve the quantitative characterisation of flow processes (ii) provide a new modelling platform and (iii) give an updated description of the groundwater flow mechanisms in the region according to the new model including the response to current and future stresses.

A range of both well-established and innovative techniques were applied, including:

- Drilling and construction of six nested groundwater observation well sites targeting the major aquifer units, including diamond coring of the Munno Para Clay at two sites, downhole wireline logging for the deepest drillhole at each site, and installation of pressure transducers and wireline piezometers
- Sampling from the newly drilled observation wells and a selection of existing bores for a range of chemical analyses, including: Major ions, stable isotopes of water, stable and radioactive carbon isotopes, strontium isotopes and (noble) gasses (Helium, Neon, Argon, and Nitrogen)
- Chloride mass balance (CMB) approach to quantify recharge across the Adelaide Plains and the western Mount Lofty Ranges
- Differential longitudinal stream gauging of Brownhill, First, Second, Third, Fourth and Fifth Creeks to establish groundwater – surface water exchange fluxes
- Steady state and transient 1D solute transport modelling of environmental isotope and ^4He concentrations through the Munno Para Clay to determine vertical hydraulic parameters and leakage
- Detailed study of the origin of dissolved salts and salinization mechanisms using new and existing data
- Field and numerical modelling approaches to examine groundwater flow dynamics across fault zones
- Estimation of transmissivity values using the tidal method and a number of analytical solutions
- Regional groundwater flow and transport modelling

The flux estimates obtained from field and desktop-based investigations were generally in good agreement with the outcomes of the regional flow model. Diffuse recharge in the Plains is an exception, being estimated to equate 0.8 % of rainfall by the CMB method and an order of magnitude less by the model (via calibration). The simplifying assumptions underlying the CMB method are numerous, but the model-based estimate is also prone to uncertainty. Additional work is required to refine the quantification of diffuse recharge in the Plains.

A new regional groundwater flow and transport model of the Adelaide Plains has been developed. Such a model is viewed as the best tool available to integrate the data as it allows accounting for all spatiotemporal constraints implied by the regional setting. The model domain extends from the major faults at the foothill of the Mount Lofty Ranges (MLR) in the south and south-east, up to 5 km offshore in the west and it is bounded by the Light River in the north. Compared to previous modelling efforts for the same area, the new platform includes the following key improvements:

- The implementation of boundary conditions relies on stronger physical basis
- The hydrostratigraphy was revised according to newest interpretation of geological data
- A sensitivity analysis was performed on grid resolution, time-step resolution and initial condition for the transient flow model and used as a guide to decide on these structural parameters
- A larger dataset for calibration was collated
- Automatic calibration (as opposed to manual calibration) was achieved; however, while the initial aim was to use hydraulic head and chemistry data as calibration targets, compatibility issues between MODFLOW-NWT and MT3DMS precluded this and thus only hydraulic head data were used
- Calibration performance was extensively assessed using relevant indicators
- Parameters sensitivity, identifiability and uncertainty were analysed
- The model was built using a script based approach, facilitating modifications

The current modelling platform is viewed as an ongoing effort towards achievement of regional-scale predictions of hydraulic heads, fluxes, Cl and ¹⁴C. It should not be expected to provide locally accurate predictions. On the basis of the SRMS (2.99 % for hydraulic heads, 28.28 % for Cl and 24.05 % for ¹⁴C), the current model can be deemed suitable for regional prediction of hydraulic head but not for Cl and ¹⁴C. The uncertainty around flux predictions is unknown and this is considered to be a major limitation. Furthermore, a number of issues were identified that warrant further work before the model can be deemed capable of providing reliable future predictions:

- Grid resolution (1,000 m) is too coarse to allow accurate estimates of groundwater-surface water exchanges
- The initial condition biases the results of the pre-development period
- A number of parameters deviated significantly from their preferred value during calibration
- Strong biases are observed in the weighted residuals of the calibration dataset

The water balance and flow mechanisms were analysed on the basis of the new model. However, given the limitations of the model, it must be kept in mind that a large uncertainty surrounds these results. The description below is hence largely subject to verification and refinement in future works.

Under pre-development conditions, the results show that both river leakage and subsurface lateral flow from the MLR contribute significantly to the inflows to the Tertiary aquifers. The results also suggest that a significant part of the flow from the MLR occurs via flow through the bedrock which subsequently feeds the Tertiary aquifers by upward flow in the Golden Grove Embayment. This potentially significant groundwater pathway does not seem to have been reported as such before. However, little data is available in deep aquifers to confirm or deny this modelling outcome and this warrants further investigation including new field work.

The model results suggest that introduction of pumping changed this balance and caused significant storage depletion, which amounts to about two thirds of the inflows to the system for the year 2012. The low calibrated value for the specific storage of both the T1 and T2 aquifers, which are the most used aquifers in the Adelaide Plains, implies that increased pumping draws the head down in these aquifers. In response, the sedimentary formations above and below provide large amounts of water to these aquifers. For a business-as-usual predictive scenario, storage loss continues into the future, but at a slightly decreasing rate as other sources start to contribute more water. The coastal boundary switches from net outflow to net inflow by 2050.

The impacts of groundwater abstraction raise a number of management questions in regard to the T1 and T2 aquifers. Given the relatively high groundwater salinity found in the Quaternary sediments above, and potentially in the T3 and T4 aquifers below where some old (> ~20,000 years), hypersaline groundwater was identified, the cross-formational flow induced by pumping as suggested by the model would imply significant risks of increase in salinity. However, the time frame over which this might become an issue for groundwater usage remains unknown, and there is currently limited evidence of increased salinity in the T1 and T2 aquifers. Groundwater has also started to flow inland from the coast according to measured hydraulic heads and to the model results. However the location of the salt water interface in the deeper confined aquifers is unknown and it may be located some distance off-shore. The model results also suggest that river leakage increased in response to abstraction, which would indicate potential adverse effects on river/wetland ecosystems; further work is nevertheless warranted to confirm this result. Future scenario modelling suggests that the storage depletion will be ongoing and therefore that the adverse effects depicted above will be intensified. If this is confirmed, further development of managed aquifer recharge (MAR) might be required to curb the ongoing declining trend.

Even though a number of steps were undertaken in this project to improve the understanding of groundwater system and the modelling platform, some key issues have been identified and call for further work before the model could be deemed suitable for making reliable future predictions including rigorous uncertainty quantification. Key recommendations for further improvement listed in this report should be implemented to achieve a better tool.

1 Introduction

The largest reserves of fresh groundwater in the Adelaide Plains are contained in the Tertiary T1 and T2 aquifers which extend from the Eden-Burnside Fault and Para Fault in the east up to an unknown distance offshore in the west (Gerges 1999). These groundwater resources have been utilised since the start of the 20th century and continue to act as a vital water resource for Adelaide's industry, agriculture and horticulture, and recreational facilities. With growing pressures such as increasing groundwater demand and a changing climate, the longevity of these resources is a critical concern, which calls for effective groundwater management. In this context, a robust understanding of groundwater flow mechanisms is required. Furthermore, a regional groundwater modelling platform is expected to provide key support as it will help scientifically-informed decisions to be made.

A modelling platform was previously developed by RPS Aquaterra (Georgiou *et al.* 2011) for the Department of Environment Water and Natural Resources (DEWNR) and has recently been used to help manage the groundwater resources of the Adelaide Plains. However, the model showed some significant contradictions with the accepted conceptualization of the groundwater flow mechanisms in the region. Namely, diffuse recharge largely dominated the water budget (Georgiou *et al.* 2011). In contrast, diffuse recharge across the Adelaide Plains is believed to be insignificant, with recharge being mainly the result of infiltration from surface water features (Miles 1952; Shepherd 1975; Gerges 1999). The model also showed groundwater flowing from the plains towards the hills along a significant portion of the eastern model boundary, especially in the North Adelaide Plains (NAP), when groundwater should globally flow from the hills towards the plains. Furthermore, the model did not benefit from a number of modern techniques available for calibration and parameter uncertainty analysis. Together these weaknesses raised concerns about the reliability of the model for use as a support tool for management.

This study aims (i) to improve the quantitative characterisation of flow processes using a range of both well-established and innovative techniques; (ii) to provide an improved modelling platform that would demonstrate a greater reliability for being used as a support tool for management; and (iii) to give an updated description of the groundwater flow mechanisms including the response to current and future stresses. To achieve these goals, a combination of approaches were applied to better characterize aquifers and aquitards properties as well as key components of the water budget, and a significant step forward was taken to improve the physical basis of the groundwater model as well as its calibration. The results of the model were subsequently analysed in detail to increase our conceptual and quantitative understanding of the groundwater resources both historically and as predicted in the future.

This summary report is based on the results of the extensive investigations as they are reported in the following Appendices:

- Appendix A: Drilling report for new groundwater monitoring wells
- Appendix B: Review of the hydrogeological properties of aquifers and aquitards
- Appendix C: Groundwater recharge estimation – chloride mass balance approach
- Appendix D: Groundwater – surface water exchange
- Appendix E: Groundwater hydrochemistry
- Appendix F: Leakage estimation across the Munno Para Clay
- Appendix G: Seawater intrusion and sources of groundwater salinity
- Appendix H: Coastal aquifer hydraulic parameter estimation based on tidal responses
- Appendix I: Determination of aquitard properties through pressure response
- Appendix J: Groundwater flow processes across fault zones
- Appendix K: Regional groundwater modelling

This report is organised in three parts. Part I presents the results of field and desktop investigations; this includes an up-to-date introduction to the hydrogeological setting of the Adelaide Plains (section 2) and

specific improvements made concerning the understanding and quantification of diffuse groundwater recharge (section 3), groundwater-surface water interaction (section 4), flow across faults (section 5) and inter-aquifer leakage (section 6). Part II describes key improvements made concerning the modelling platform (section 7), presents the capabilities and limitations of the new model (section 8) and gives model-based estimates of water balances in pre-development, development and future periods (section 9). Finally, part III provides an integrated discussion of the project outcomes (section 10), a revised description of the groundwater flow mechanisms in the region (section 11), an overview of possible implications for resource management (section 12) and key recommendations (section 13).

Part I Field and Desktop Investigations

2 Hydrogeological setting

2.1 Geology

Geologically, the Adelaide Plains is part of the St Vincent Basin which extends beneath the Gulf St Vincent and is bounded to the east by the Mount Lofty Ranges (Figure 1). Cainozoic sediments have been deposited in sub-horizontal sequences of widely ranging grain size (i.e. clay to gravel). These sedimentary sequences are bounded below and in the east by the Proterozoic fractured rocks of the Barossa Complex and Adelaidean groups. These fractured rock units form the Western Mount Lofty Ranges that are part of the Adelaide Geosyncline (Figure 1). The boundaries between the sedimentary sequences and the fractured rock are largely defined by a series of major faults. The most notable are the Eden Burnside and Para faults which bound the Adelaide Plain sub-basin and Golden Grove Embayment, respectively. For more detail, the reader is referred to Gerges (1999).

2.2 Hydrostratigraphy

The sedimentary aquifer system of the Adelaide Plains is made up by a complex arrangement of Tertiary and Quaternary age units with a total thickness of up to several hundreds of metres. In the Northern Adelaide Plains (NAP), the Quaternary sediments have been generalised into a series of six aquifers (Q1-Q6), which are confined by six layers of low permeability sediments (Cb1-Cb6). Southward towards the Torrens River in the Central Adelaide Plains (CAP), these aquifers partly merge together and are generally only treated separately west of the Para fault. The Quaternary aquifers and aquitards are not as clearly delineated in the Golden Grove Embayment (GGE) and are generally undifferentiated. From a broad hydrostratigraphic perspective, all the Quaternary sediments in the Adelaide Plains are often lumped together into one single unit called the Hindmarsh Clay, which has the role of an aquitard (Zulfic *et al.* 2008). The underlying Tertiary sediments have been classified into the first, second, third and fourth Tertiary aquifers (referred to as T1, T2, T3 and T4 respectively). The extent of the Tertiary sediments offshore is unknown, and therefore it is also unknown whether or not they outcrop at a certain distance offshore.

The first Tertiary aquifer (T1) is comprised of a range of sediment types including for example the Hallett Cove Sandstone, Dry Creek Sand, Carisbrooke Sand, and the limestone of the Upper and Lower Port Willunga Formation, depending on where it is encountered (Gerges 2006; Zulfic *et al.* 2008). The aquifer is confined by overlying Quaternary sediments, except where it outcrops within the Golden Grove Embayment between the Hope Valley and Eden Burnside faults and just east of the Para fault (Figure 2). The T1 aquifer is underlain by the Munno Para Clay which acts as an aquitard for the T2 aquifer. The T2 aquifer is comprised primarily of the Lower Port Willunga Formation limestone and occasionally the sandy facies of the Aldinga Member (of the Port Willunga Formation) and the Chinaman Gully Formation. The aquifer covers only part of the Golden Grove Embayment, but extends northward past the Gawler River and presumably beyond the northern limit of the Northern Adelaide Plains Prescribed Wells Area (Figure 2). The T2 aquifer overlays the Blanche Point Formation which consists of clay, siltstone and marl sediments. The latter acts as an aquitard for the underlying T3 and T4 aquifers, which are comprised of the South and North Maslin Sands. A synthetic presentation of the stratigraphy and hydrostratigraphy of the area is shown in Table 1. Cross-sections through the Central Adelaide Plains and Golden Grove Embayment are shown in Figure 3, while Figure 4 provides a three-dimensional overview of the main hydrostratigraphic units, based on the most recent interpretation of borehole data (unpublished data provided by DEWNR during the course of the project).

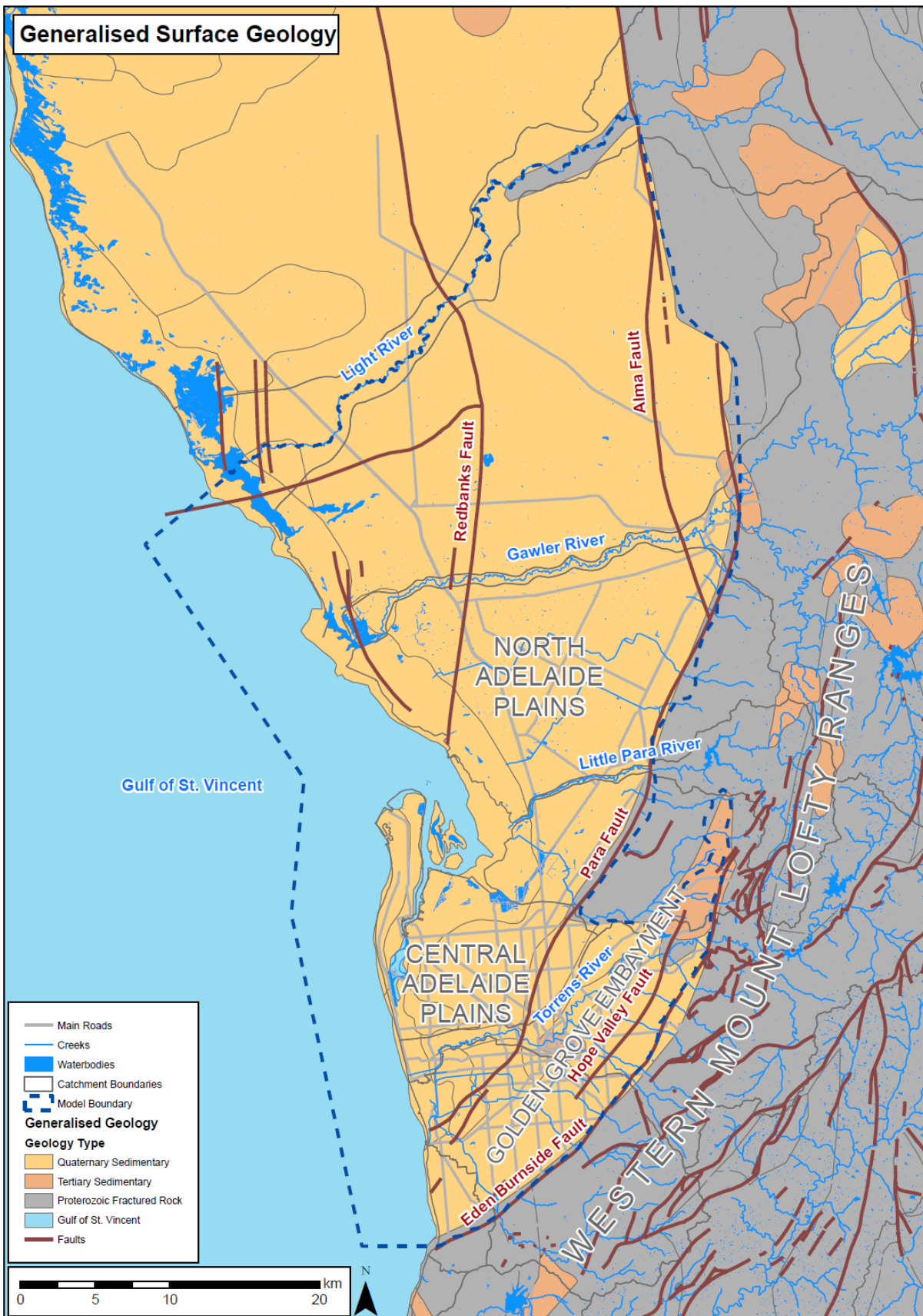


Figure 1 Generalised geology showing the Northern and Central Adelaide Plains, Western Mount Lofty Ranges and the numerical groundwater model boundary

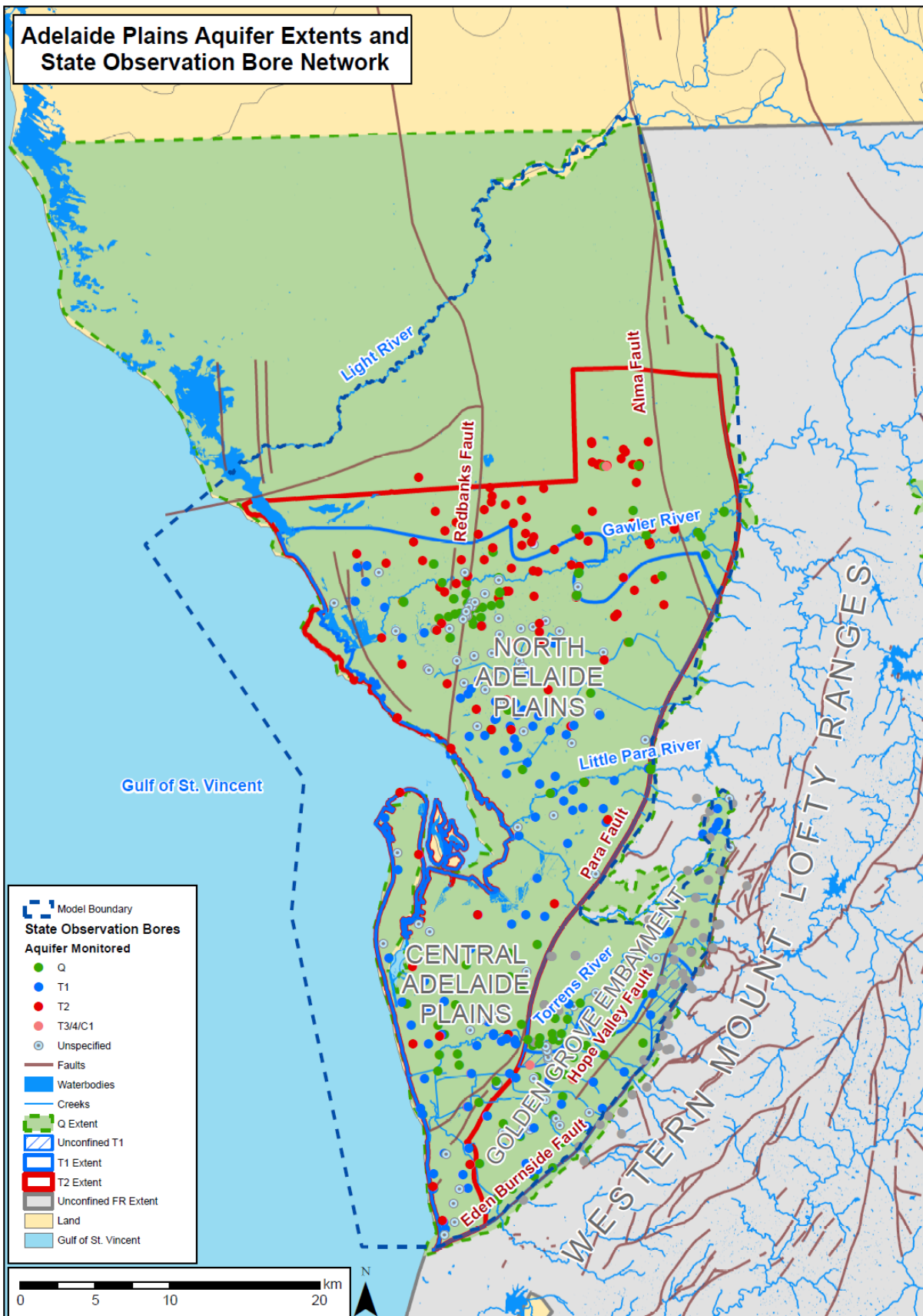


Figure 2 Generalised hydrogeology showing the Quaternary, T1, T2 and Fractured Rock aquifer extents in addition to the currently operational State Observation Bore Network. Note that the indicated northern bounds of the Quaternary and T2 aquifers are the boundaries of the Prescribed Wells Area; the aquifers do in fact extend further north

Table 1 Stratigraphy and hydrostratigraphy of the Adelaide Plains (Zulfic *et al.* 2008)

Age	Golden Grove Embayment			Adelaide Plains Sub-Basin					
	Stratigraphy	Hydrostratigraphy	Description	Stratigraphy	Hydrostratigraphy	Description			
Quaternary	Holocene	Semaphore Sand, modern alluvium and beach gravels	Unconfined Aquifer	Thin sand aquifers restricted mainly to coastal areas	Semaphore Sand, modern alluvium and beach gravels	Unconfined Aquifer	Thin sand aquifers near coast		
		Saint Kilda Formation	Unconfined Aquifer	Thin sand, shell aquifers near coast					
Pleistocene	Pooraka Fmn	Aquitard		Pooraka Fmn	Aquitard				
	Keswick Clay	Aquitard		Keswick Clay	Aquitard				
	Hindmarsh Clay	Aquitard, Q1–Q5 Aquifers	Mainly clay aquitard with interbedded sandy aquifers	Hindmarsh Clay	Aquitard, Q1–Q6 Aquifers	Mainly clay aquitard with interbedded sandy aquifers			
Pliocene?	Carisbrooke Sand	T1 Aquifer	Carisbrooke Sand Aquifer	Thin sandy mainly confined aquifer with restricted extent	Carisbrooke Sand	Carisbrooke Sand Aquifer	Confined sandy aquifer, most significant in eastern side of NAP PWA		
Pliocene	Hallett Cove Sandstone and Dry Creek Sand		T1a Aquifer	Thin sandy confined aquifer restricted to western areas	Dry Creek Sand	T1 Aquifer	T1a Aquifer	Confined sandy aquifer, thickening to the south-west	
	Croydon Facies		Semi-confining bed	Croydon Facies				Semi-confining bed	
Tertiary	Miocene to Oligocene	Upper Limestone	T1b Aquifer	Confined aquifer, mainly limited to area between Para Fault splinters	Upper Limestone	T1b Aquifer	Confined aquifer, thickening to south and south-west		
		Munno Para Clay Member		Aquitard	Confining bed limited to western areas		Munno Para Clay Member	Aquitard	Confining bed, absent in north of NAB PWA
		Lower Limestone	Undifferentiated Sand	T1 or T2 Aquifer	Confined aquifer, extent limited to south-west areas	Lower Limestone	T2 Aquifer	Thick confined aquifer, sandy and thinning in north and north-east of NAB PWA	
		Ruwarung Member		Aquitard	Mainly confining bed	Ruwarung Member		Aquitard	
		T1 Aquifer		Restricted extent					
	Aldinga Member	Aquitard		Clay unit	Aldinga Member	Aquitard		Clay unit	
	Eocene	Chinaman Gully Formation		T2a or T3 Aquifer	Variable sand	Chinaman Gully Formation		T3 Aquifer	Sand unit
			Aquitard	Clay unit			Aquitard and T3 Aquifer	Mainly confining bed, minor thin sandy aquifer	
Blanche Point Fmn		Aquitard	Confining bed		Blanche Point Fmn	Aquitard	Confining bed		
Tortachilla Limestone		T3–T4 Aquifer	Thin confined aquifer		Tortachilla Limestone	T4 Aquifer	Thin confined aquifer		
South Maslin Sand			Thin confined aquifer, thickest in the east		South Maslin Sand				
Clinton Formation		Aquitard	Confining bed, restricted extent		Clinton Formation	Aquitard	Confining bed, restricted extent		
North Maslin Sands	T3–T4 Aquifer	Thin confined sandy aquifer		North Maslin Sands	T4 Aquifer	Confined sandy aquifer			

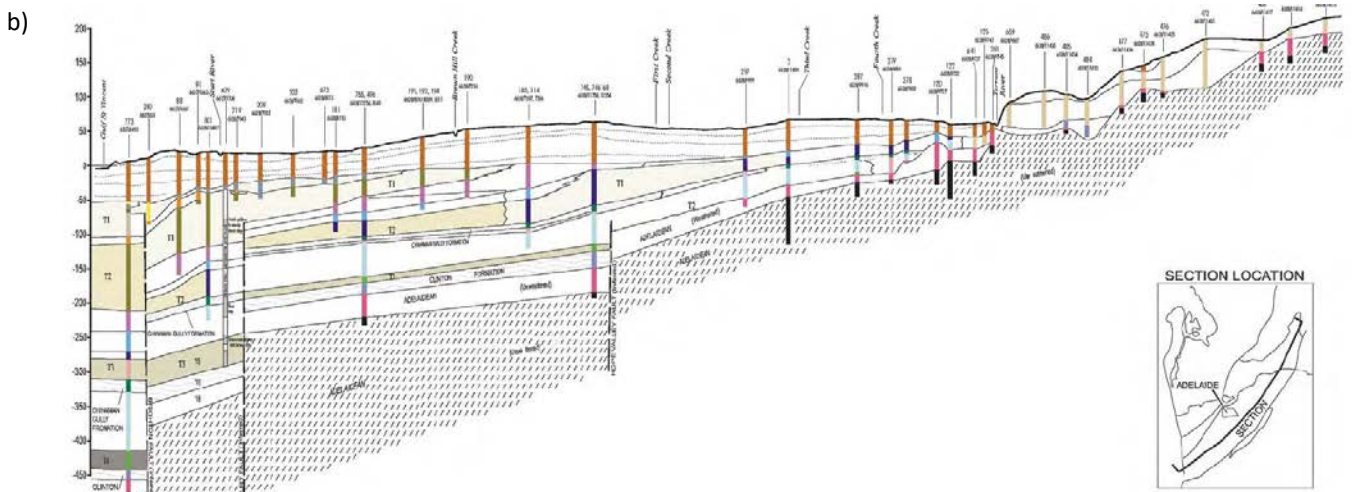
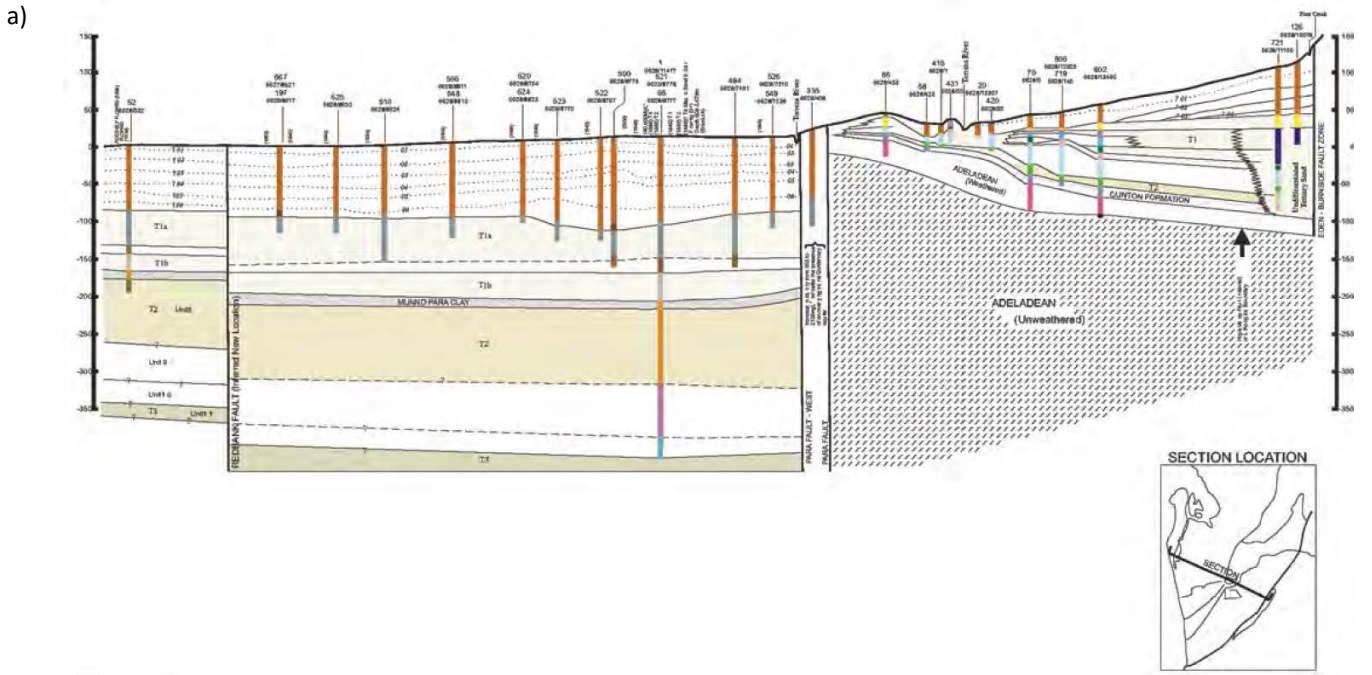


Figure 3 Cross-sections through the Central Adelaide Plains and the Golden Grove Embayment (Gerges 1999).

Hydrostratigraphic units

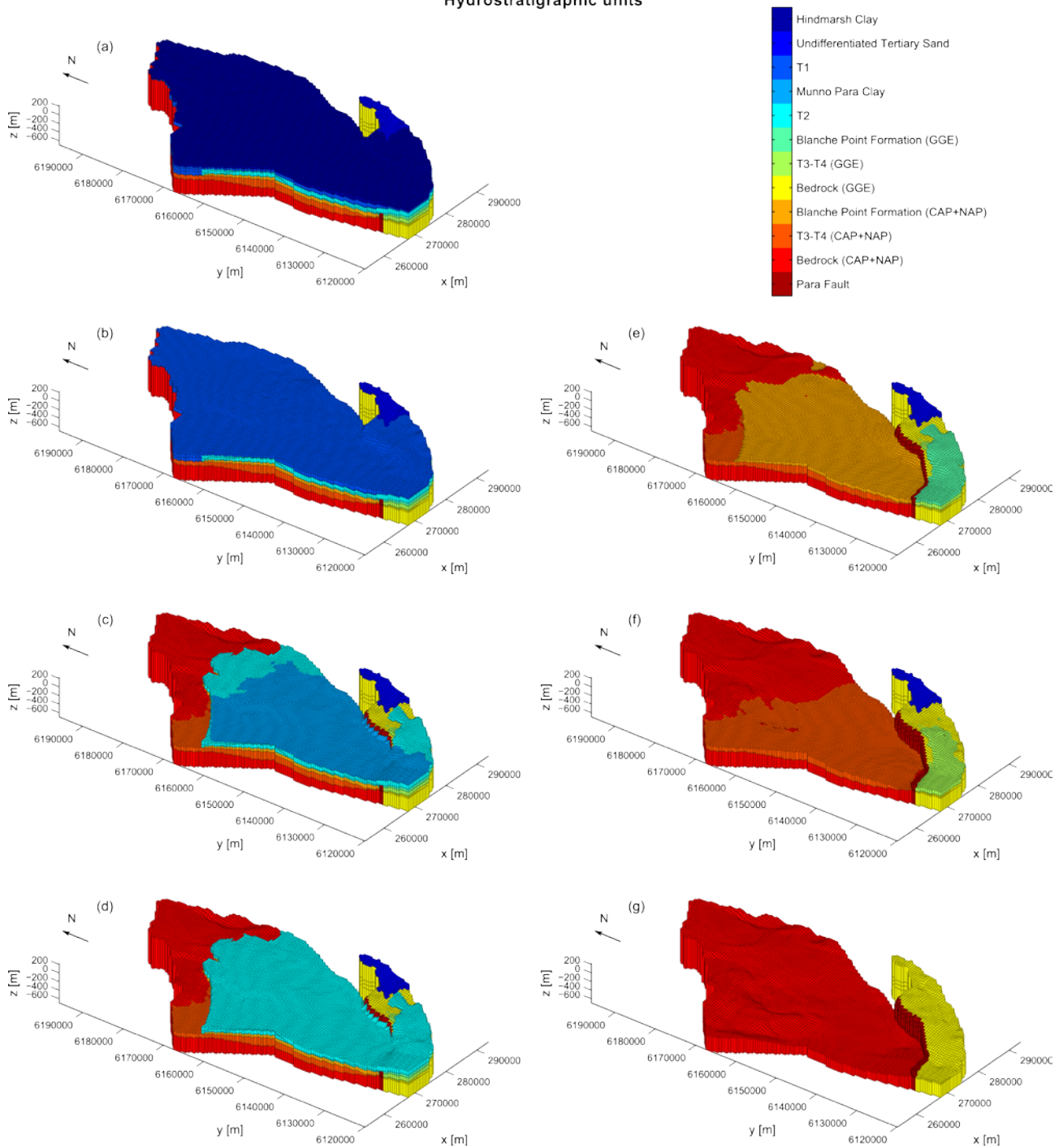


Figure 4 Three-dimensional visualisation of the hydrostratigraphic units used in the numerical groundwater model (vertical exaggeration x10). One or several units are removed (starting from the shallowest) from Figure (a) through to Figure (g), making the deeper units visible

2.3 Aquifer and aquitard properties

The most comprehensive overview of the hydraulic properties of the aquifers and aquitards is provided by Gerges (1999), Gerges (2006) and Hodgkin (2004). A comprehensive description of all studies to date and summary tables of hydraulic property values can be found in Appendix B. Additional values of the hydraulic conductivity and the storage coefficient of various units have been derived within the current study using environmental tracers (Appendix F), a tidal method (Appendix H) and vibrating wire piezometers (Appendix I). Table 2 provides a condensed overview of all available values and shows that the horizontal and vertical hydraulic conductivity (K_h and K_v , respectively) and the specific storage (S_s) typically vary by 2 to 3 orders of magnitude within a single aquifer or aquitard unit. These parameters are representative of aquifer properties across a range of spatial scales depending on the methods used to derive them. They should be considered with caution when upscaled to represent regional properties. For example, estimates of K_v based on hydraulic tests of core samples often underestimate the regional scale value of K_v , which is required in the numerical model, as they do not necessarily capture preferential pathways. Additionally, aquifer tests evaluate K_h and S_s values that are representative of the aquifer in the vicinity of a well (i.e. tens to hundreds of meters), while values derived using the tidal method or pressure responses in vibrating piezometers are representative of much larger areas.

Table 2 Summary of vertical hydraulic conductivity (K_v), horizontal hydraulic conductivity (K_h) and specific storage (S_s) values determined from hydraulic tests on core samples or from in-situ pumping (after Gerges (1999), Gerges (2006) and Hodgkin (2004) in addition to values derived in this study). Q stands for Quaternary, T for Tertiary

	Q AQUIFERS	Q AQUITARDS	T1 AQUIFER	MUNNO PARA CLAY	T2 AQUIFER
K_v (m day ⁻¹)	Range	5.1E-07 – 3.4E-03		1.5E-07 – 5.3E-05	
	Median	4.3E-05		1.7E-06	
	Mean	3.1E-04		6.4E-06	
	Standard Deviation	6.7E-04		1.1E-05	
	Number of Values	62		21	
K_h (m day ⁻¹)	Range	5.6E-06 – 6.0E-03	1 – 120	1.3E-06 – 8.1E-06	1 – 45
	Median	6.0E-05	3.6	2.8E-06	2.7
	Mean	6.3E-04	9.4	3.7E-06	6.7
	Standard Deviation	1.6E-03	21.7	2.5E-06	10.1
	Number of Values	16	41	5	19
S_s (m ⁻¹)	Range	9.8E-05 – 6.0E-05	7.3E-05 – 1.8E-03	8.1E-06 – 1.3E-05	2.8E-05 – 1.1E-03
	Median	1.6E-05	3.4E-04	1.1E-05	1.6E-04
	Mean	2.6E-05	4.9E-04	1.1E-05	3.3E-04
	Standard Deviation	2.1E-05	4.8E-04	2.6E-06	4.0E-04
	Number of Values	4	9	2	5

2.4 Groundwater salinity

Salinity maps were constructed by collating all available most recent electrical conductivity measurements from the WaterConnect database. Only bores with aquifer information were selected, supplemented by bores that were less than 30 m deep to be classified for our purposes as representative of the Quaternary aquifers (see Appendix C for more detailed methodology and results). This resulted in over 20 000 electrical conductivity measurements. The distribution of groundwater salinity based on interpolation of these data points reveals clear spatial patterns in the shallow aquifers (Figure 5). Lower salinity groundwater is observed in the vicinity of the Gawler and Little Para Rivers in the north, as well as near the ephemeral creeks flowing into the Golden Grove embayment. Groundwater salinity in the T1 and T2 aquifers shows broad areas of both higher and lower salinity (Figure 6). Much of the low salinity groundwater appears to be roughly aligned with major surface water features (e.g. Gawler, Little Para and Torrens Rivers).

Hypersaline groundwater has been reported in the Adelaide Plains, mainly in the T3-T4 aquifers (Gerges 1999). Little is known about the origin of this water, and attempts during this project to collect water samples of it for further analyses were unsuccessful. A detailed study in the Willunga Embayment (Appendix G) has shown, however, that hypersaline groundwater is encountered in equivalent hydrostratigraphic units. The formation of this hypersaline water is most likely related to dry climatic conditions in the past. Based on the similarity of the ionic ratios calculated from hydrochemical concentration data of existing wells, it could be established that the hypersaline groundwater in the Adelaide Plains and Willunga Embayment are genetically related (Figure 7). It also appears that mixtures of the hypersaline groundwater and freshwater occur in the T1, T2 and fractured rock aquifers at several locations across the Adelaide Plains. Insufficient data were available to assess the status of seawater intrusion to the Tertiary aquifers.

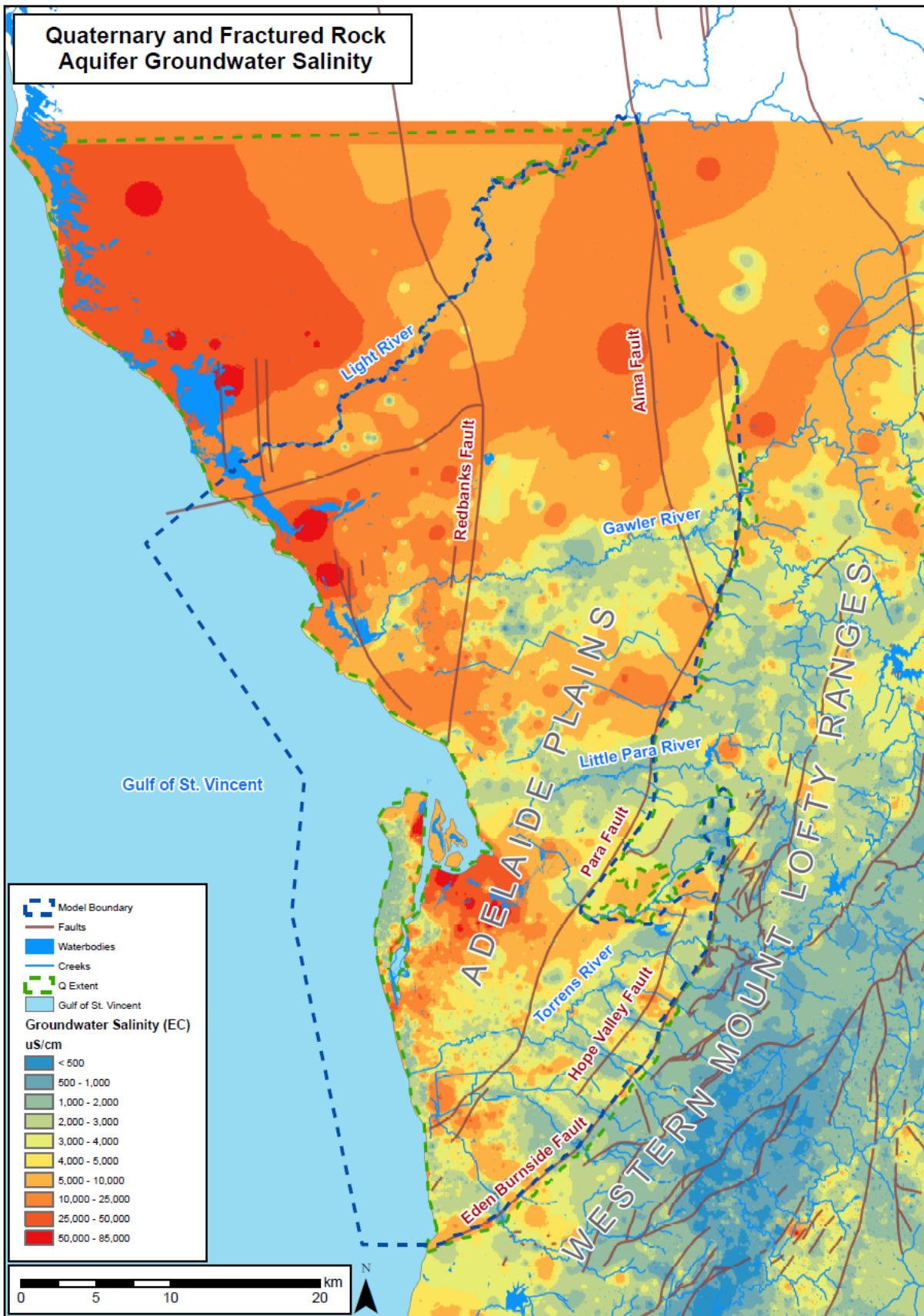


Figure 5 Most recent groundwater salinity (expressed in units of electrical conductivity EC) for Quaternary aquifers (and additionally bores whose maximum drilled depth was between 0 m and 30 m) and Fractured Rock aquifers at any depth

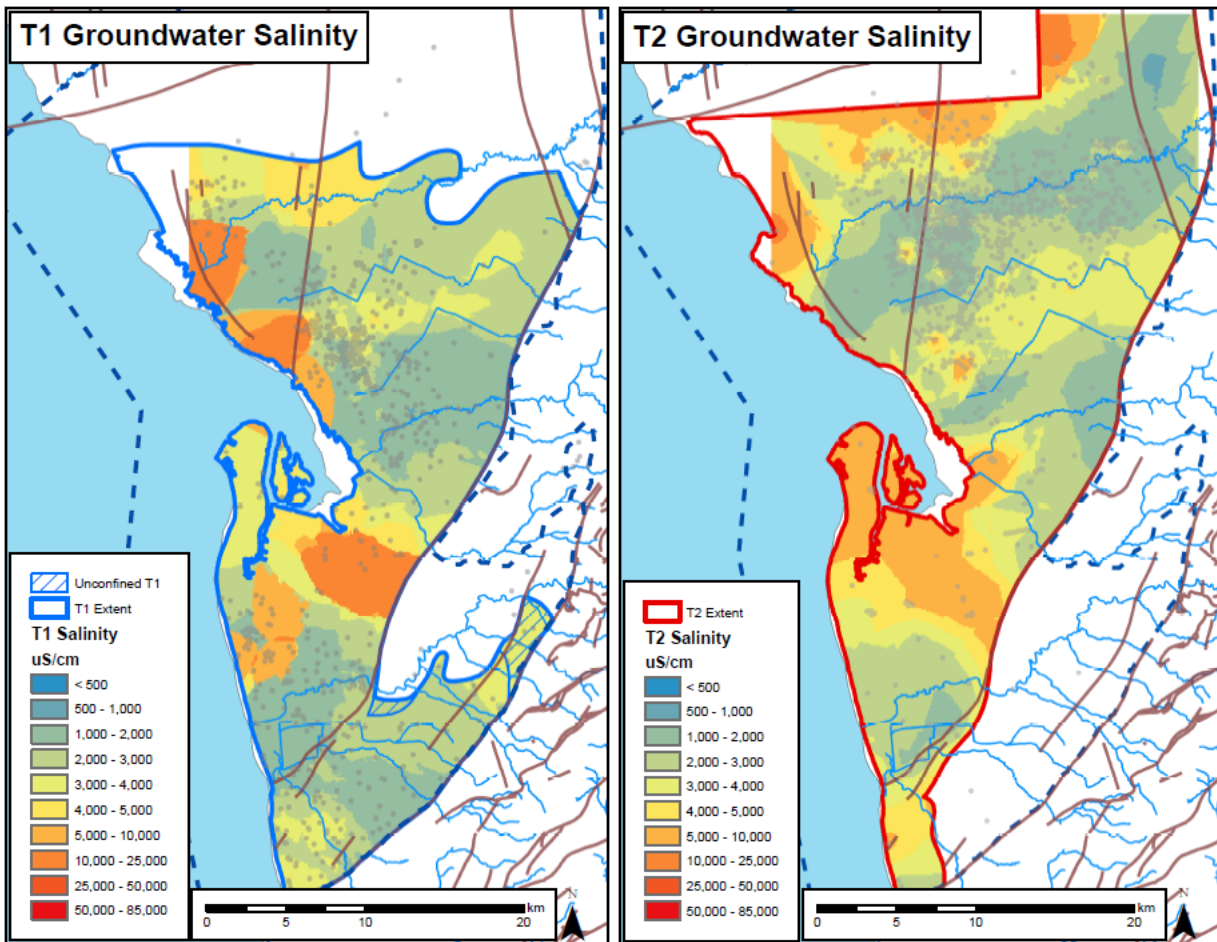


Figure 6 Most recent groundwater salinity (expressed in units of electrical conductivity EC) for T1 and T2 aquifers shows broad corridors of good quality groundwater in much of the study area in both aquifers

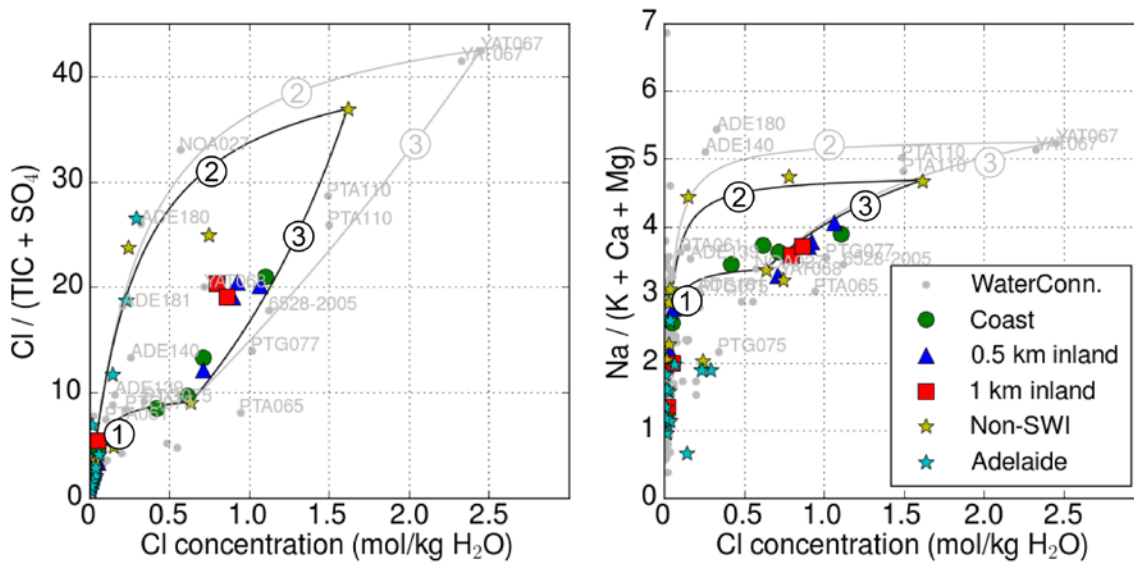


Figure 7 Graphs showing (left) the ratio of $\text{Cl} / (\text{TIC} + \text{SO}_4)$ versus the chloride concentration and (right) the ratio of $\text{Na} / (\text{K} + \text{Ca} + \text{Mg})$ versus the chloride concentration. Ratios are based on concentrations expressed in meq L^{-1} . Numbered lines represent the relationships resulting from mixing between freshwater and seawater (1), freshwater and hypersaline water (2) and seawater and hypersaline water (3). Black lines are based on the most saline sample from the Willunga area (WLG096), grey lines are based on the most saline sample from the Adelaide Plains area (YAT067). Coloured symbols except cyan stars represent samples from the Willunga Embayment (see appendix G for details), grey symbols are data points for the Adelaide Plains area obtained from the WaterConnect database. Cyan stars represent samples obtained in the new observation wells drilled for this study (Appendix E)

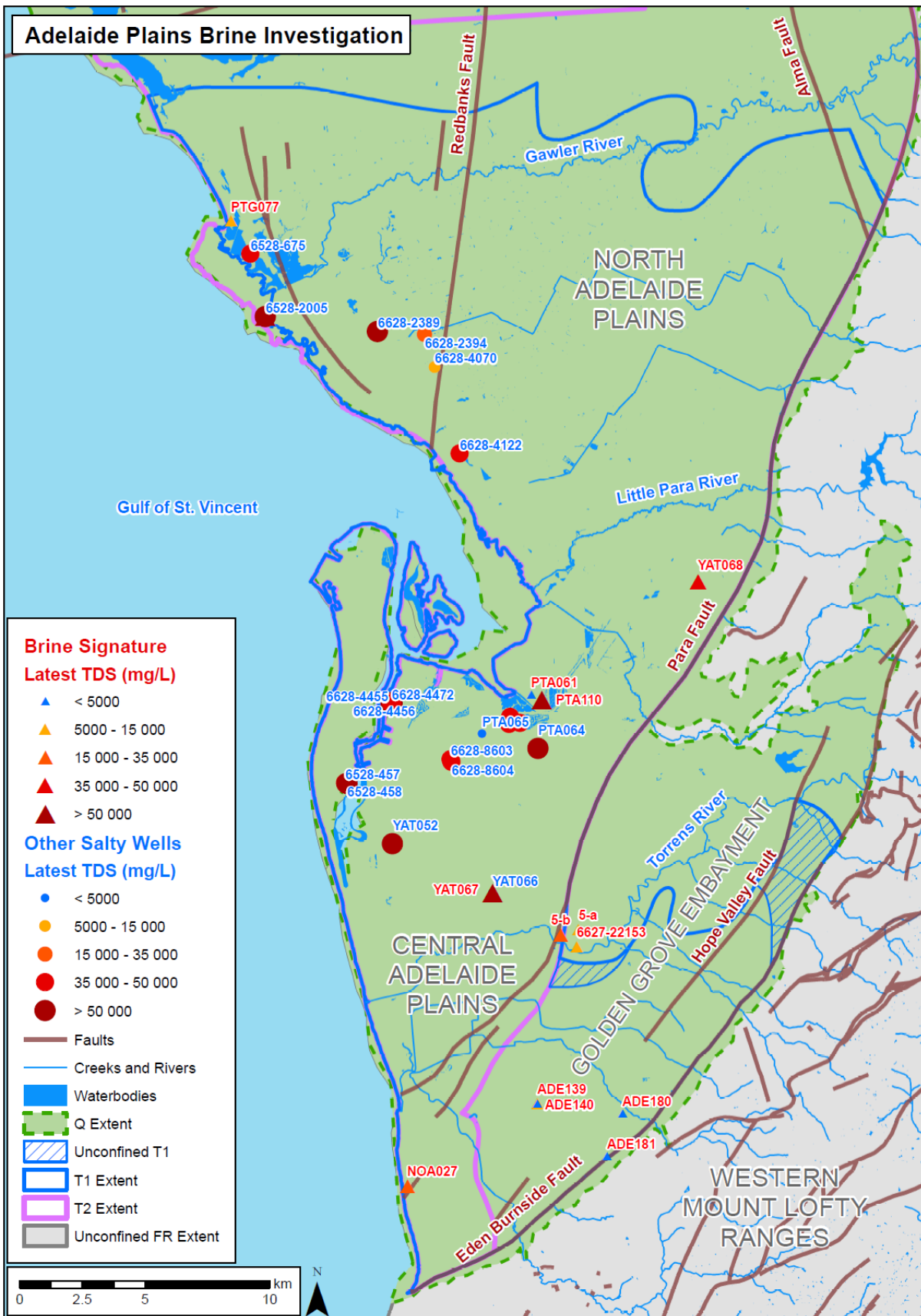


Figure 8 Locations of saline groundwater across the Adelaide Plains with size and shape indicating salinity (mg L^{-1}). Marker symbol indicate if sample has a hydrochemical signature of hypersaline water (triangles) or unknown (circles). The samples span different aquifers but are mostly from the T3, T4 and FRA aquifers, and were taken between 1966 and 2005

2.5 Groundwater potentiometric surfaces

Groundwater levels in unconfined aquifers are expected to follow a subdued form of the topography and are likely to be influenced by reservoir, river or creek infiltration where those surface water features are losing to the underlying aquifers (Winter *et al.* 1998). Groundwater generally flows northeast to southwest and from east to west in the Adelaide Plains sub-basin and Golden Grove Embayment respectively. The potentiometric surfaces of the confined and semi-confined aquifers are influenced by historical and current groundwater extraction. The pre-development potentiometric surfaces of the T1 and T2 aquifers were artesian suggesting the potential for upward flow into the Quaternary aquifers (Smith 1979; Gerges 2001). Large cones of depression have then formed in the Northern and Central Adelaide Plains as a result of extensive pumping in the T1 (Figure 9) and T2 (Figure 10) aquifers. Consequently, potentiometric surfaces are now well below sea level across large areas (Zulfic 2002; Zulfic *et al.* 2008; Baird 2010) and there are significant downward hydraulic gradients that indicate downward flow into the Tertiary aquifers from overlying units. Fewer groundwater bores have been drilled and maintained in the T3-4 aquifers and so less information is available for these aquifers. However, there is a risk that the drawdowns created in the T2 and T1 aquifers may lead to salinization, either from the overlying Quaternary units or underlying hypersaline aquifer. The time frame over which this might become an issue for groundwater usage remains unknown.

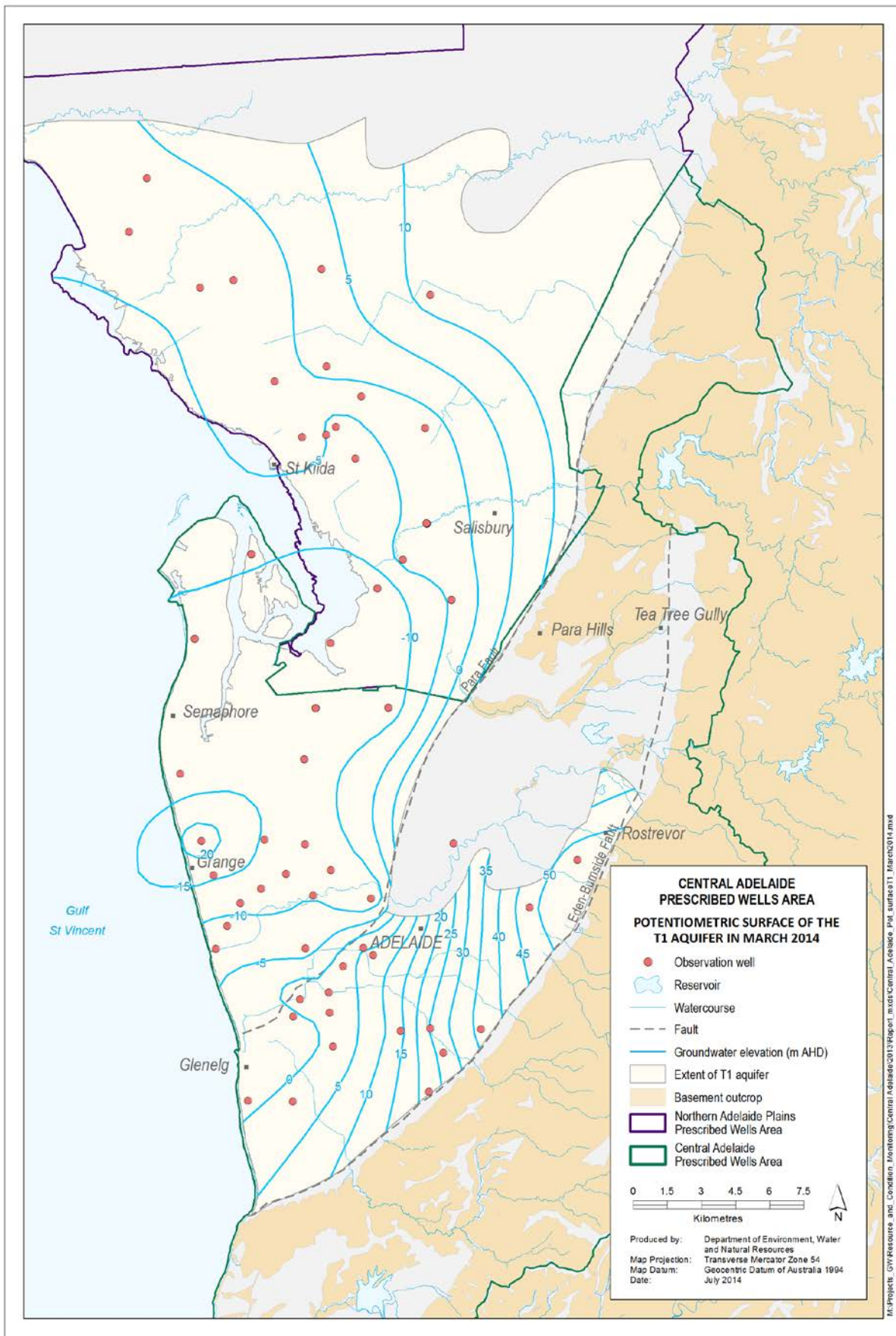


Figure 9 Potentiometric surfaces for the T1 aquifer in March 2014 (courtesy of DEWNR)

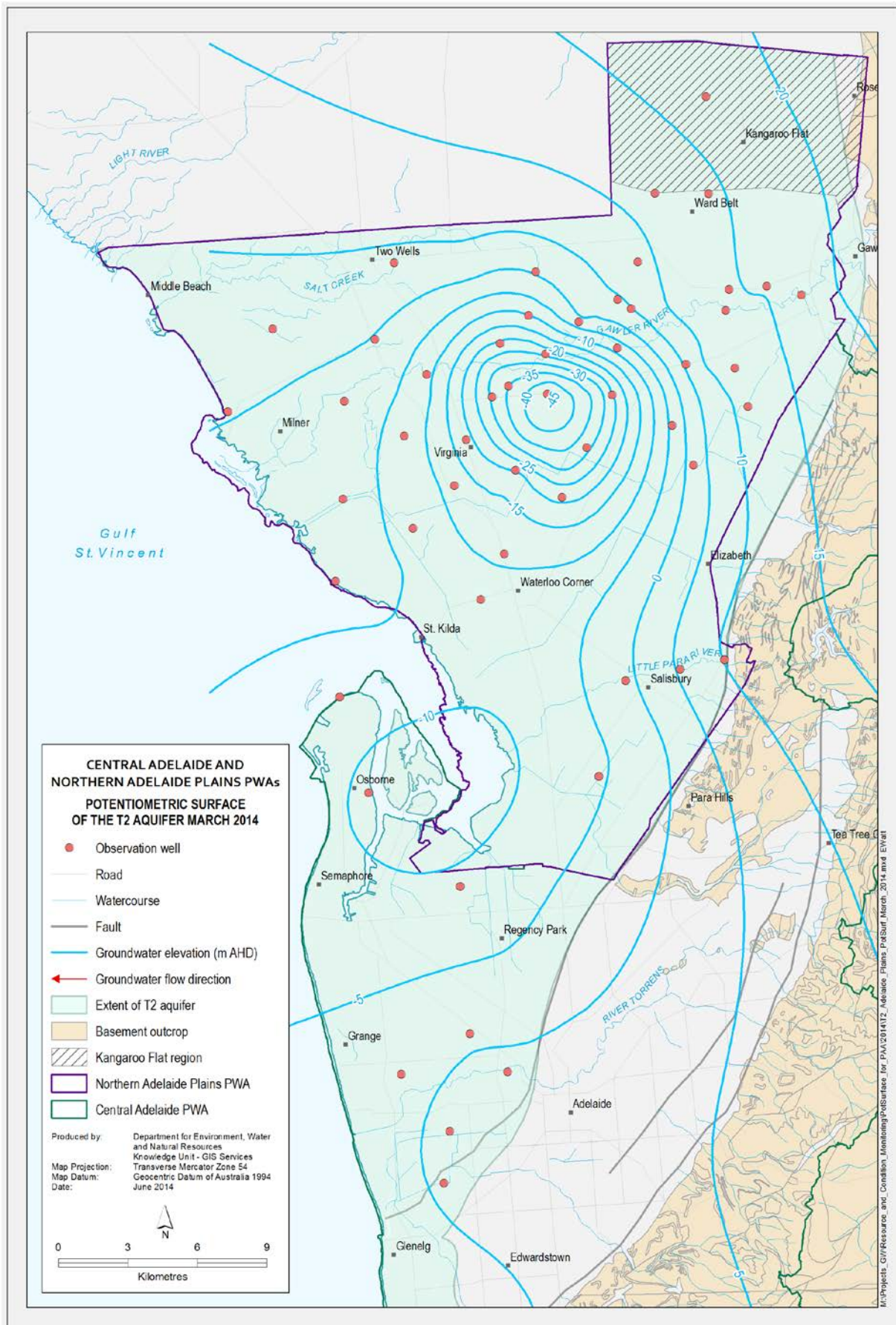


Figure 10 Potentiometric surfaces for the T2 aquifer in March 2014 (courtesy of DEWNR)

2.6 Groundwater use

Groundwater use across the Adelaide Plains primarily occurs from the T1 and T2 aquifers as their salinity and yields are generally better than the shallower Quaternary aquifers. Groundwater extraction has increased since it was first used in the early 1900s for a range of purposes but primarily for the irrigation of market gardens, supplementary drinking water supplies and production by beverage companies (Gerges 1999). The total pumping across the region in 2011 was estimated to be 32 GL yr⁻¹ according to data provided by Georgiou *et al.* (2011).

Managed aquifer recharge (MAR) schemes have been operational in the Adelaide Plains for some decades, with a number of now well established schemes (e.g. Bolivar). The total current injection rate is estimated to be 8.5 GL yr⁻¹ (unpublished data supplied by DEWNR). The locations of the schemes that are operational, in construction or under investigation are also shown in Figure 11 and amounts 23 GL yr⁻¹. The vast majority of these are located in the Northern Adelaide Plains and are located across a vast area.

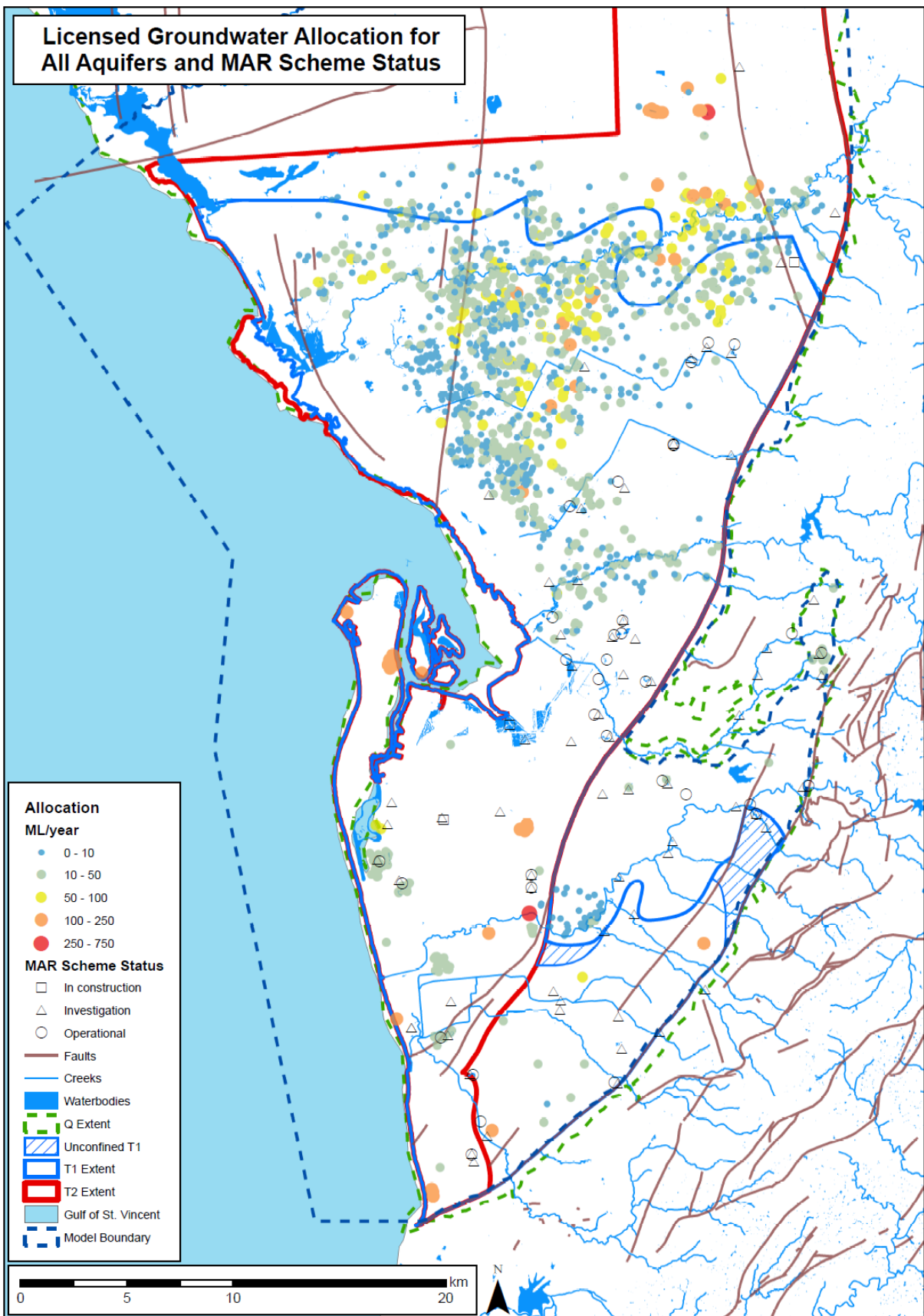


Figure 11 Current licensed groundwater allocation for all aquifers in the NAP and CAP in addition to MAR scheme location and status

3 Diffuse groundwater recharge

3.1 Introduction

Diffuse recharge across the Plains is believed to be insignificant, with infiltration being principally sourced from surface water features (Miles 1952; Shepherd 1975; Gerges 1999). Despite that, a diffuse recharge rate equal to 5 % of rainfall was applied in the previous model by Georgiou *et al.* (2011). This resulted in a large dominance of diffuse recharge in the water budget, thus contradicting the previous understanding of recharge mechanisms of the aquifers in the area. This recharge rate was based on a former model by REM (2006b) which included the MLR as part of the model domain. In that model, this recharge rate was applied based on recharge estimates for the MLR, and not for the Plains (REM 2006a). As significantly less rainfall occurs in the Plains than in the MLR, a recharge rate of 5 % of rainfall is likely to be an overestimation of diffuse recharge across the Plains.

No estimate of diffuse recharge across the Plains was in fact found in the literature. In order to fill this gap, diffuse recharge was estimated in this project using the chloride mass balance (CMB) method, as described in detail in Appendix C. The method was also applied to quantify diffuse recharge across the Western MLR, but the results are summarized below for the Plains only.

3.2 Chloride mass balance approach

The CMB method resulted in a median recharge estimate of 3.6 mm yr⁻¹ for the Quaternary aquifers, i.e., 0.8 % of rainfall given the average rainfall over the model area for the period 1889–2013 (438 mm yr⁻¹). Across the model domain, this represents a total recharge of 6.1 GL yr⁻¹.

An important limitation of the approach is that groundwater in the Quaternary aquifers can partly originate from the MLR via lateral flow into the Tertiary aquifers and subsequent upward flow. Historical groundwater flow (i.e., prior to heavy pumping) was indeed upward from the T1 aquifer into the Quaternary aquifers over large areas, as suggested by hydraulic heads (Gerges 1999; 2001). As groundwater in the MLR is generally fresher (Figure 5), corresponding groundwater samples would bias the result towards an overestimation of diffuse recharge. Leakage from streams into the Quaternary aquifer can also bias the CMB method. As stream water would generally be fresher than diffuse recharge, this can once more bias the result towards an overestimation. Moreover, direct surface runoff was neglected, which can also imply overestimation. A final cause for overestimation is the potential effect of sampling bias, as most wells are drilled into the freshest parts of the Quaternary aquifers, which favours the prevalence of higher recharge rates. Other uncertainties arise from assumptions on rainfall chloride concentration and rainfall amount estimates, which both were considered uniform over the area, with unknown implications on the result.

4 Groundwater-surface water interaction

4.1 Introduction

The western draining creeks of the Mount Lofty Ranges flow ephemerally across the Adelaide Plains. Due to the downward hydraulic gradients between the creeks and the underlying aquifers west of the Eden Burnside Fault and Para Fault, they are likely to provide a considerable source of recharge to the Quaternary aquifers (Miles 1952; Gerges 1999; 2006). Shepherd (1975) and Hutton (1977) estimated river leakage from the Little Para River to be 2.35 and 2.1 GL yr⁻¹ respectively (using the water table fluctuation method and a differential stream gauging method, respectively). Teoh (2006) found loss rates of 1.37 GL yr⁻¹ for Brownhill Creek and suggested large losses from the Sturt River based on hydrological modelling. Green *et al.* (2010) estimated river leakage from creeks flowing across the Eden Burnside Fault using differential stream gauging. They found losing conditions for Brown Hill Creek, First Creek and Fifth Creek across the Eden Burnside Fault, with estimated volumes of 0.5, 0.3 and 0.09 GL yr⁻¹, respectively, and gaining conditions for Second Creek, Third Creek and Fourth Creek.

The current study further quantified the groundwater – surface water exchange rates for creeks flowing across the Eden Burnside Fault using differential stream gauging with better spatial and temporal resolutions (Appendix D). The results of this approach are summarized below.

4.2 Differential stream gauging approach

Differential stream gauging was carried out in 2014–2015 on the basis of dilution gauging. The measurements confirmed the previously-proposed general model of gaining conditions upthrown and losing conditions downthrown of the fault (Gerges 2006; Green *et al.* 2010; Currie *et al.* 2011). Brownhill Creek and First – Fifth Creek were all found to show losing average conditions across or past the Eden Burnside Fault. Spatial and temporal variability (Figure 12 and Figure 13) can explain differences with the results of Green *et al.* (2010), in particular concerning Second – Fourth Creek which were found to show losing conditions by Green *et al.* (2010). Head differences between the creeks and the underlying aquifers west of the Eden Burnside Fault also suggest that streams are losing near the Fault. Finally, electrical conductivity data also suggest clear gaining conditions upthrown of the Eden Burnside Fault and a decrease or an absence of groundwater discharge to streams downthrown of the Fault.

When adjusted for riparian evapotranspiration (0.93 L s⁻¹ km⁻¹ – assuming 4 mm day⁻¹ over a 20 m wide riparian zone), the average loss rates for Brownhill Creek and First – Fifth Creek downstream of the fault range from 2 to 6.1 L s⁻¹ km⁻¹ during baseflow conditions. This equates to approximately 1.3 GL yr⁻¹ of river recharge assuming that these rates occur for 6 months of the year along 3 km of creek length westward from the Eden Burnside fault. It is likely that this represents a conservative value of river recharge because loss rates can be higher during periods of high flow (Cranswick *et al.* 2015).

When the same exchange rates are extrapolated to the Sturt, Little Para and Gawler Rivers, together these ephemeral surface water features add approximately 4.7 GL yr⁻¹ of leakage to the Quaternary aquifers. Caution must be taken when considering this regional scale estimate though, as such a rough upscaling necessarily introduces considerable uncertainty. Furthermore, a number of surface water features such as Dry Creek, Cobbler Creek, Smith Creek, Light River, lakes and farm dams were not included in this calculation.

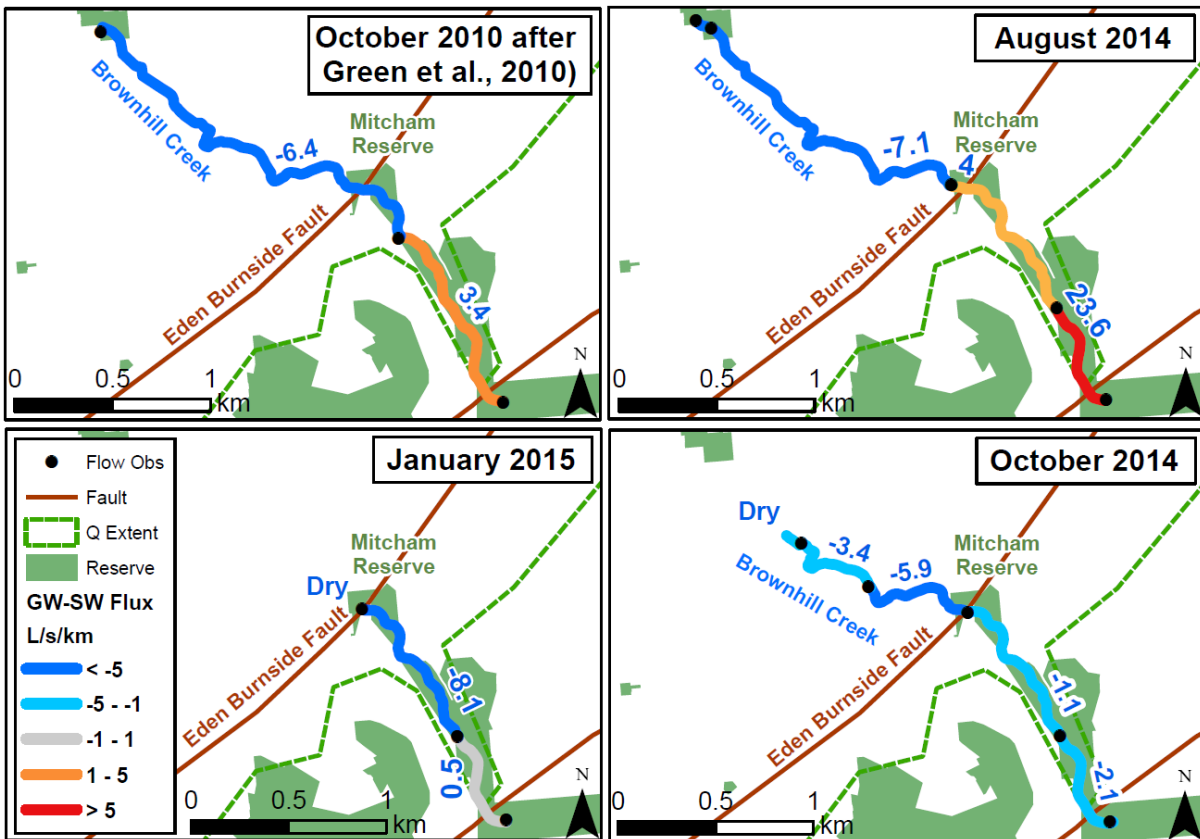


Figure 12 Groundwater – surface water exchange rates for Brownhill creek at four separate gauging times show generally consistent trends of losing conditions below the fault and gaining conditions above the fault. Temporal variability in exchange flux is thought to be due to the changing hydraulic head gradients between the creek and underlying/adjacent aquifers in time. Black circles indicate gauging locations and creek flow direction is from southeast to northwest

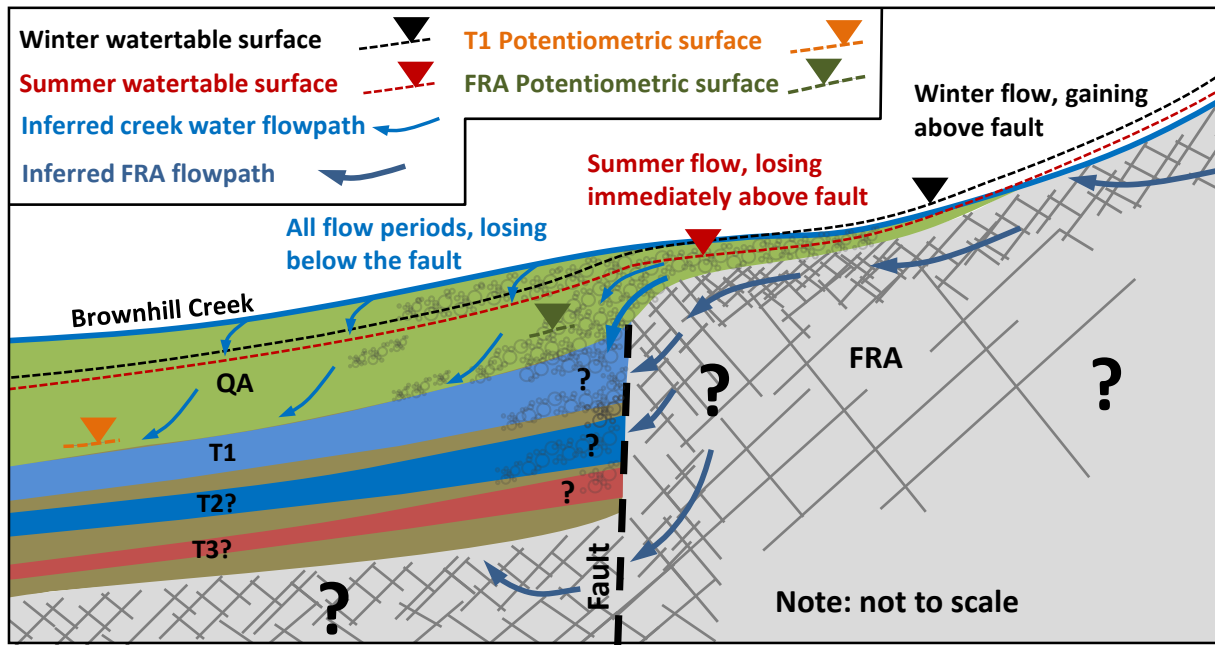


Figure 13 Conceptual model of groundwater flow and groundwater – surface water exchange in the vicinity of Brownhill Creek

5 Flow across the faults

5.1 Introduction

The widely adopted conceptual model presented by Gerges (1999) suggests that the Tertiary aquifers are predominantly recharged by lateral flow from the Fractured Rock aquifers to the east. Several geophysical studies (Leaf *et al.* 2012; Manning *et al.* 2012) have been done across the Adelaide Plains to describe the structure, orientation and displacement of the major fault systems but these surveys do not discuss the geological controls of such features on groundwater flow. A study by Green *et al.* (2010) investigated the likely mechanisms and rates of groundwater flow across the Eden Burnside Fault into the Adelaide Plains aquifers. Their study suggested that groundwater may flow directly across the fault from the fractured rock aquifer into the sedimentary aquifers through “zones of breakage”. Green *et al.* (2010) also hypothesised that an indirect pathway for groundwater from the fractured rock aquifer to the sedimentary aquifers is via the surface water features that traverse the fault zone and contribute via river leakage to the shallow sedimentary aquifers.

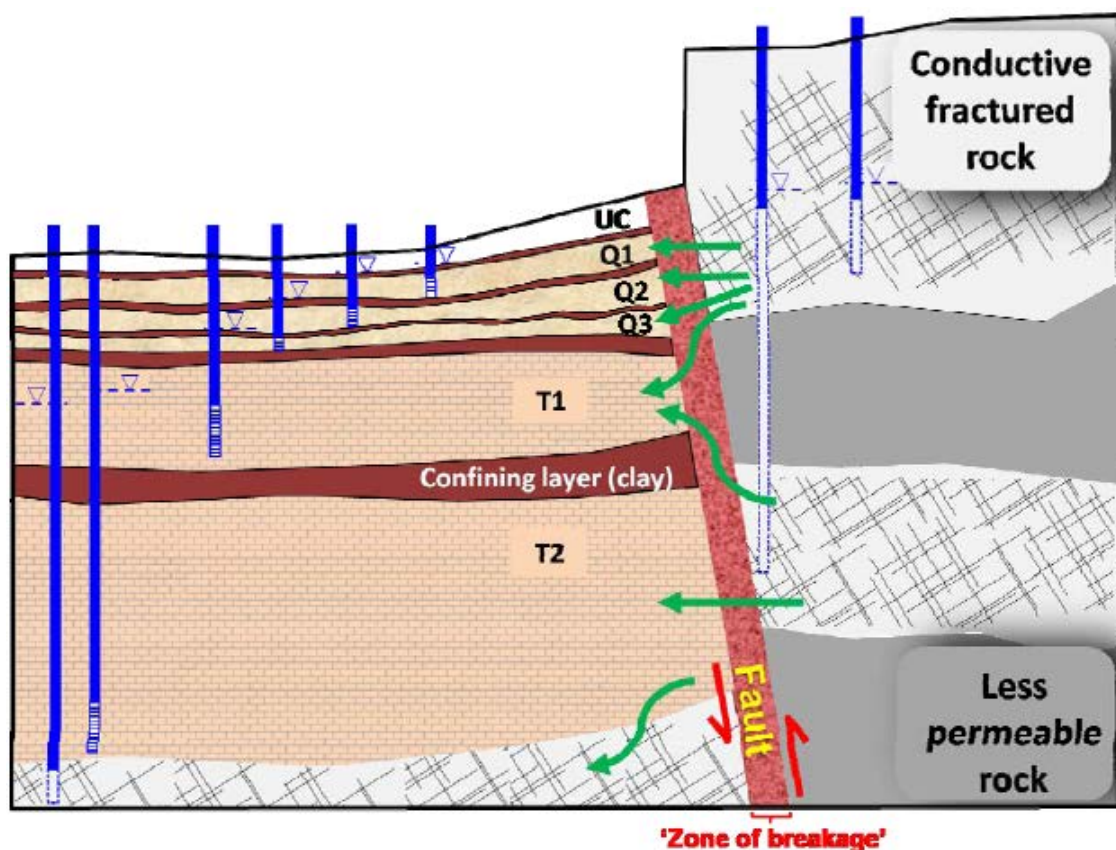


Figure 14 Conceptual model of flow across the Eden-Burnside Fault (after Green *et al.* 2010)

In the vicinity of the fault zone, groundwater levels can be much higher above the fault than they are below the fault. Near 5th creek for example, there is an 80 m fall in groundwater level over a distance of 353 m between bores ADE133 and ADE147 (Figure 15). The fact that hydraulic head gradients across the fault zone are much higher than those further away suggests that the fault could represent a low-permeability feature. As this appears to be in contradiction with previous findings, this study looked at different environmental tracers to investigate the regional flow dynamics across the Adelaide Plains, including flow across the fault. Groundwater samples were taken along three main cross-sections, as detailed in Appendix E and summarized below.

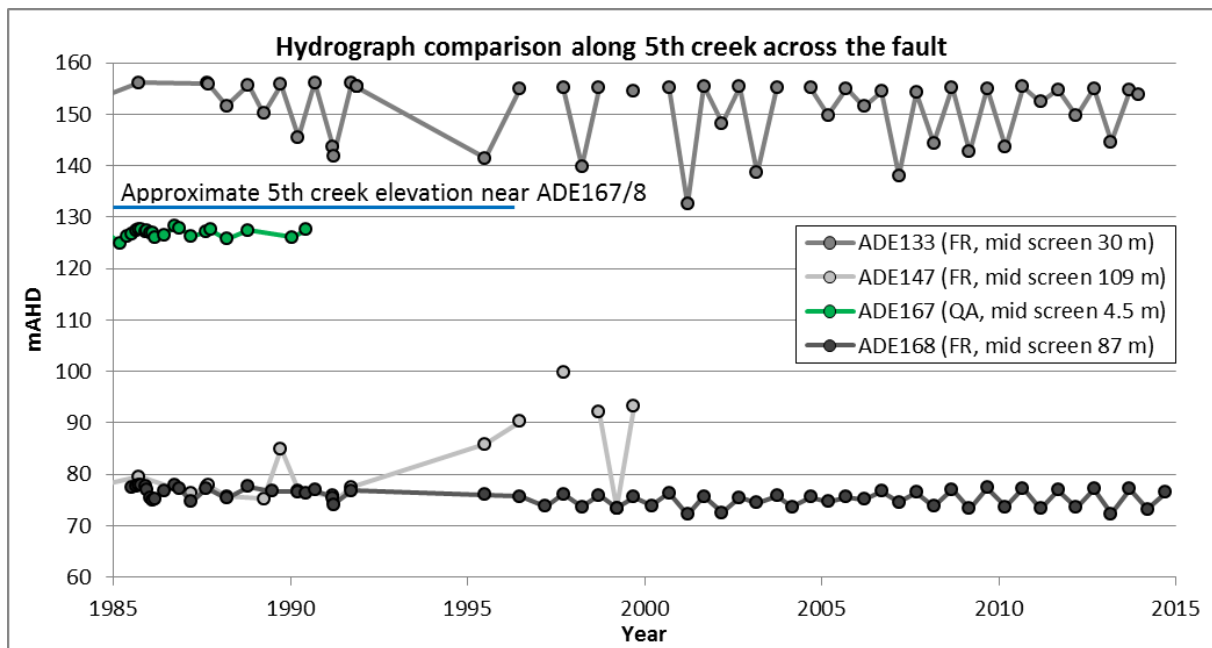


Figure 15 Hydrograph comparison for Fractured Rock aquifer monitoring bores east and west of the Eden Burnside fault along 5th creek. The horizontal distances between ADE133 east of the fault and ADE147 and ADE168 west of the fault are 353 and 697 m respectively.

5.2 Geochemical analysis

It was found that within the main Tertiary aquifers, the ¹⁴C activity decreases with depth and with distance from the Mount Lofty Ranges. This is most apparent along the central and southern transects in the T1 aquifer and along the northern transect in the T2 aquifer. Along the northern transect, the increase in age with distance from the MLR indicates a mean flow velocity of 1.1 m yr⁻¹. The ¹⁴C values could be fitted by assuming a constant flow velocity in the T2 aquifer, which would be consistent with a model in which most of the water originates from the Mount Lofty Ranges and that recharge from overlying layers does not add much water along the flow path (as this would lead to an increase of the flow velocity in the T2 aquifer if its hydraulic properties and thickness are spatially uniform). Along the southern transect, the groundwater flow velocity within the T1 aquifer appears to decrease west of the Para Fault (Figure 16): Between the Eden-Burnside Fault and the Para Fault the mean flow velocity based on ¹⁴C values is 0.6 m/year, while west of the Para Fault, a flow velocity of 0.2 m yr⁻¹ is inferred. The decrease in flow velocity could be partly due to an increase in aquifer thickness, or it could reflect upward flow from the Tertiary into the Quaternary aquifer.

It is noteworthy that some very high ¹⁴C activities (i.e. young ¹⁴C ages) were measured close to the Para Fault in the north and the Eden-Burnside Fault in the south. A ¹⁴C activity of 89 pmC was measured in MPA140 (T2), located between the Para and Alma Faults on the north transect and screened from 112 to 125 m below ground, and a ¹⁴C activity of 83 pmC was measured in ADE138 screened from 277 to 287 m below ground in the fractured rock immediately west of the Eden-Burnside Fault on the central transect. This is interpreted as an indication for downward movement of groundwater across the faults, and suggests that this flow may occur at significant depth. By contrast, some of the groundwater at the base of the Tertiary aquifers close to the fault is relatively old (> 30,000 yr based on measured ¹⁴C activities). This likely indicates that this water has travelled significant distances within the MLR before reaching the Para Fault and that recharge occurs over a large area. If recharge were to occur over only a relatively small area, much less variation in groundwater age with depth would be observed.

Based on the distribution of apparent ¹⁴C ages in the T2 aquifer along the northern transect, both the flow rate across the fault and the aquifer recharge rate within the MLR (where the water originates) were estimated using a simple cross-sectional model. Recharge rates within the Mount Lofty Ranges are thus calculated to be between 11 and 15 mm yr⁻¹, which is in remarkable agreement with the CMB-based

estimate of 8 – 16 mm yr⁻¹ (Appendix C). Estimated volumetric flow rates from the MLR to the plains range between 33 and 65 m³ yr⁻¹ m⁻¹. Assuming negligible lateral variation of the flow rates along Para and Eden-Burnside faults this equates to a total flux between 2 × 10⁶ and 4 × 10⁶ m³ yr⁻¹ (2 – 4 GL yr⁻¹).

As the apparent ages of the groundwater samples are up to 35,000 years, it is certain that recharge conditions have varied tremendously over this timespan due to long-term variations in rainfall (Cohen et al., 2011). Therefore, this estimate represents a long-term average, and thereby considerable uncertainty is introduced in assuming that it is representative for current conditions. The assumption that the flow rates are spatially constant along the faults also introduces large uncertainty when upscaling to the regional scale.

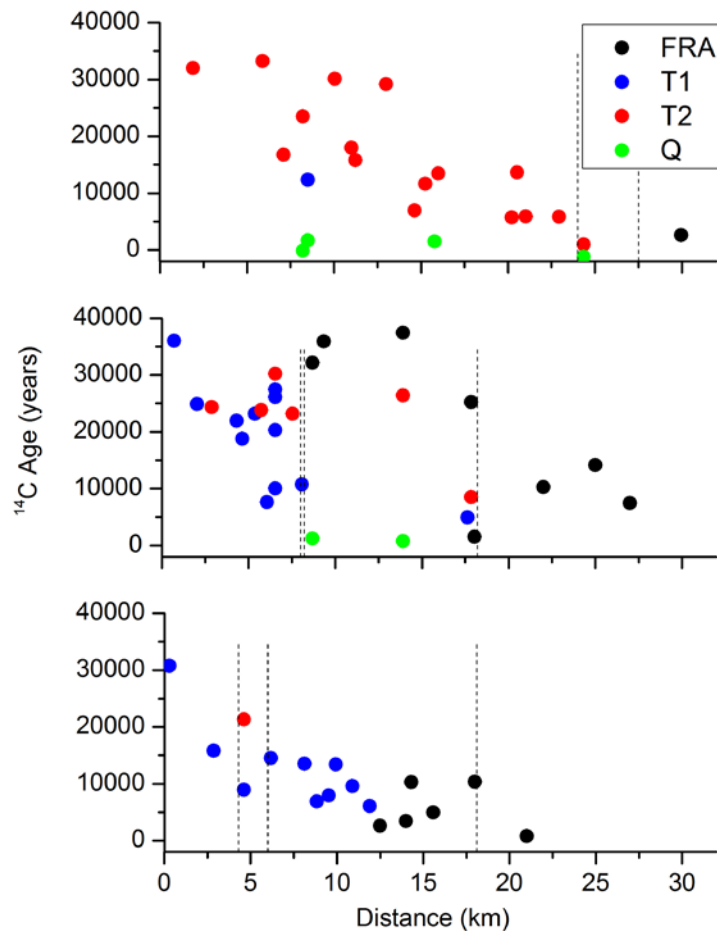


Figure 16 Carbon-14 ages along the North, Central and South Transects (top, middle and bottom respectively) show increasing age towards the coast (0 km) for the T1 and T2 aquifers with dashed lines indicating the location of faults

5.3 Comparison to the Willunga Embayment

A recent drilling project in 2012 (as part of the NCGRT Willunga Super Science program) to investigate groundwater flow processes across fault zones in the Willunga Embayment provides an analogue to the likely groundwater flow mechanisms across major fault systems within the Adelaide environment.

Groundwater flow across the Willunga Fault from the fractured rock aquifer to the sedimentary aquifers was examined at three sites within the Willunga Embayment. Hydrogeological and hydrogeophysical techniques were used to site, design and construct a series of multi-level wells up to 300 m below ground level on either side of the Willunga fault. The observed hydraulic gradients across the fault zone were very significant (up to 2.5, with a head difference of 80 m over a horizontal distance of less than 30 m).

Groundwater age dating and residence time tracers (carbon-14 and helium-4) showed that the groundwater within the fractured rock aquifer system was typically much younger than the groundwater

within the Port Willunga Formation and Maslin Sands aquifers and generally had a higher salinity. Recent sampling studies (unpublished data 2014) show that creeks carry water with similar hydrochemical characteristics as the fractured rock aquifer system across the fault, and so differentiating between groundwater flow and surface flow across the fault based on water chemistry is likely to be difficult.

A three-dimensional numerical model showed that despite the fault zone acting as a dominantly barrier-type system, approximately 1.7 to 42 % of the groundwater recharge occurring upstream of the fault zone to the fractured rock aquifer is likely to make its way across the fault. Using the range in measured head gradients across the fault and the range of fault zone hydraulic conductivities as determined by the modelling (1.7×10^{-4} to 2.7×10^{-5} m day⁻¹), the annual flux along the length of fault is in the range of 2.6 to 62 m³ y⁻¹ m⁻¹, i.e. very similar to what is found for the North Transect within the Adelaide Plains (33 - 65 m³ yr⁻¹ m⁻¹).

6 Leakage through the Munno Para Clay

6.1 Introduction

Inter-aquifer leakage can be a very important groundwater flow process at the regional scale, but there is usually little information to quantify this process. In the Adelaide Plains, inter-aquifer leakage rates need to be known because groundwater resources are in high demand and there needs to be an understanding of how processes including injection and pumping in a given aquifer will affect the adjacent aquifers. If inter-aquifer leakage is occurring at a significant rate, water resources can be over-allocated, contaminated, or degraded by other processes resulting from poor management. With an understanding of leakage rates, groundwater flow models can be calibrated to accurately represent the complex layered aquifer systems. This can lead to more effective resource management.

In this study, we aimed to quantify inter-aquifer leakage in the Adelaide Plains Sub-basin using environmental tracers. Due to the large extraction rates from the T1 and T2 aquifers, the focus of this study is on the Munno Para Clay aquitard that separates these two aquifers. To constrain rates of inter-aquifer leakage, hydrochemical analysis was combined with solute transport modelling, as detailed in Appendix F and summarized below.

6.2 Vertical hydraulic conductivity and leakage estimates

Environmental tracers were used to determine rates of inter-aquifer leakage through the Munno Para Clay at two locations. During the drilling of new wells in Welland and Gillman, core samples were collected for the analysis of helium, chloride and stable water isotopes. The distributions of these tracers were used to estimate the flux across the aquitard by calibrating the velocity in solute transport modelling (Figure 17). Based on helium data it is estimated that the flux is less than 1 mm yr^{-1} , from which it follows that the vertical hydraulic conductivity is less than $3.4 \times 10^{-6} \text{ m day}^{-1}$. Using this value in combination with the current T1-T2 hydraulic gradient map (Figure 18) a volumetric rate of upward leakage in the CAP of 366 ML yr^{-1} and downward leakage in the NAP of 1190 ML yr^{-1} is obtained.

It must be emphasised, though, that these are expected to be maximum values as they were calculated using the upper limit of hydraulic conductivity. Significant uncertainty also arises due to limitations related to recent transient conditions and to the fact that the regional scale extrapolation is based on two core-based estimates of the vertical hydraulic conductivity.

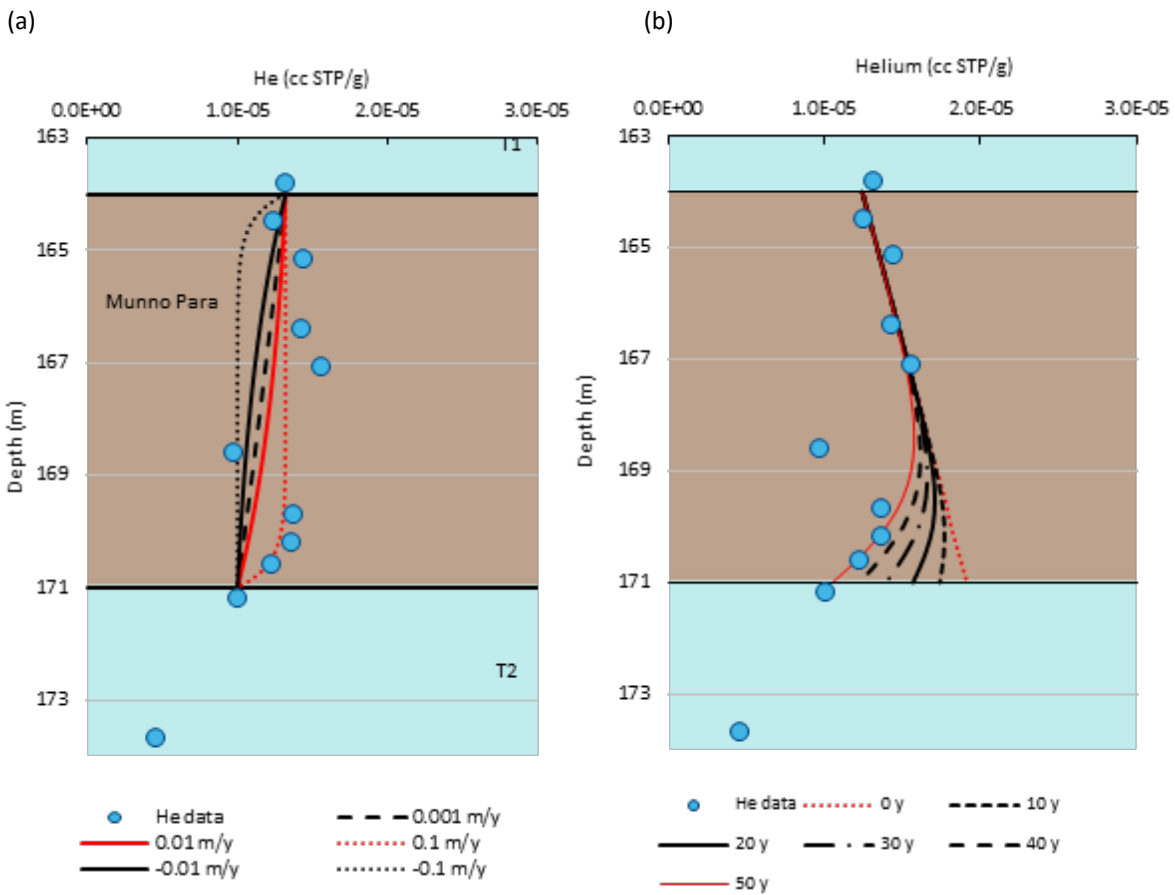


Figure 17 Site 13 modelled helium concentrations for (a) Scenario 1 and (b) Scenario 3 – further discussed in Appendix F

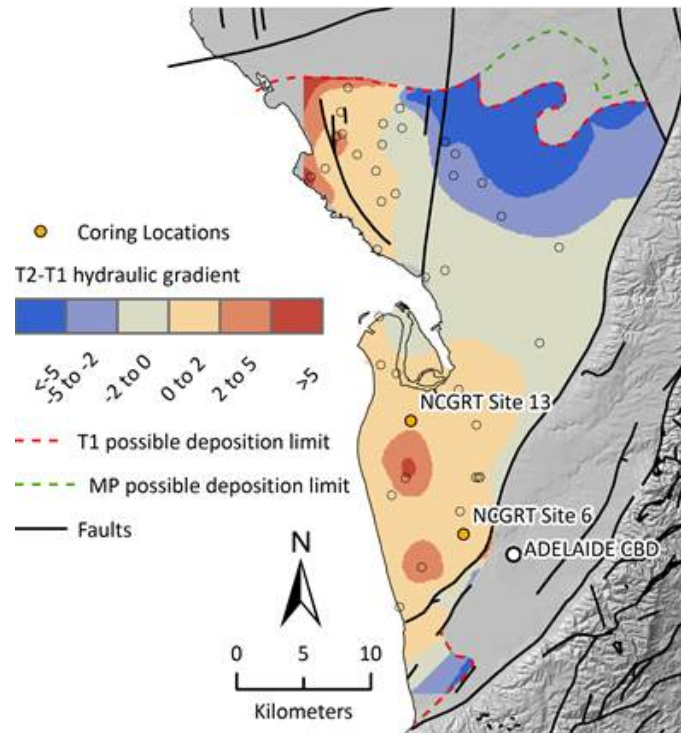


Figure 18 Year 2014 hydraulic head difference map between the T2 and T1 aquifers (units of metres), constructed using different sources and a Bayesian Data Fusion approach (details given in Appendix F). A negative difference implies downward leakage and positive difference implies upwards leakage

Part II Regional Groundwater Modelling

7 Model setup and calibration

A new regional groundwater flow and transport modelling platform was developed for the Adelaide Plains region. Such a platform is intended to provide a regional understanding of the water balance and of the impact of extraction/injection on the groundwater system. It is not intended to provide answers to local questions regarding individual wells. It could nonetheless be used to assign the boundary conditions of refined, local models. The model is based on MODFLOW-NWT for flow and on MT3DMS for transport simulations. Compared to previous modelling efforts for the same area (Georgiou *et al.* 2011), the new platform includes the following key improvements:

- The implementation of boundary conditions such as general head boundary conditions and rivers relies on stronger physical basis.
- A revision of the hydrostratigraphy. The T1 and T2 aquifers are considered continuous across Para fault and layers below the T2 aquifer were added down to and including the Bedrock.
- A sensitivity analysis was performed on the grid resolution, time-step resolution and initial conditions, and was used as a guide to decide on these structural parameters.
- A larger dataset for calibration was collated.
- Automatic calibration was used to achieve optimal parameter values.
- Calibration performance was extensively assessed using relevant indicators.
- Parameter sensitivity, identifiability and uncertainty were analysed.
- The model was built using a script based approach, which facilitates modifications.

The setup of the models is described in detail in Appendix K and summarized below for the flow models.

7.1 Model extent and hydrostratigraphy

The model domain extends from the major faults at the foothill of the MLR in the south and east, up to 5 km offshore in the west and it is bounded by the Light River in the north (Figure 19a). The model implements a simplified but comprehensive hydrostratigraphy of the area, including the main aquifers and aquitards down to and including the Bedrock. The Para Fault that separates the Golden Grove Embayment and the Adelaide Sub-Basin is explicitly represented by a line of cells extending vertically from the Blanche Point Formation down to and including the Bedrock. The top and bottom elevations of the layers are based on the hydrostratigraphy (Figure 19b). The top of the Blanche Point Formation aquitard, of the T3-T4 aquifer and of the Bedrock are implemented in different layers upthrown and downthrown of Para Fault to reflect the discontinuity in elevation across the fault. Zonation coinciding with the hydrostratigraphic units was used for assigning hydraulic and transport properties to model cells (i.e., material properties are constant within each zone). The properties were based on estimates where available (Table 2) and on literature values otherwise. In total, the model features 10 layers for 12 hydrostratigraphic units (or zones) as indicated in Table 3.

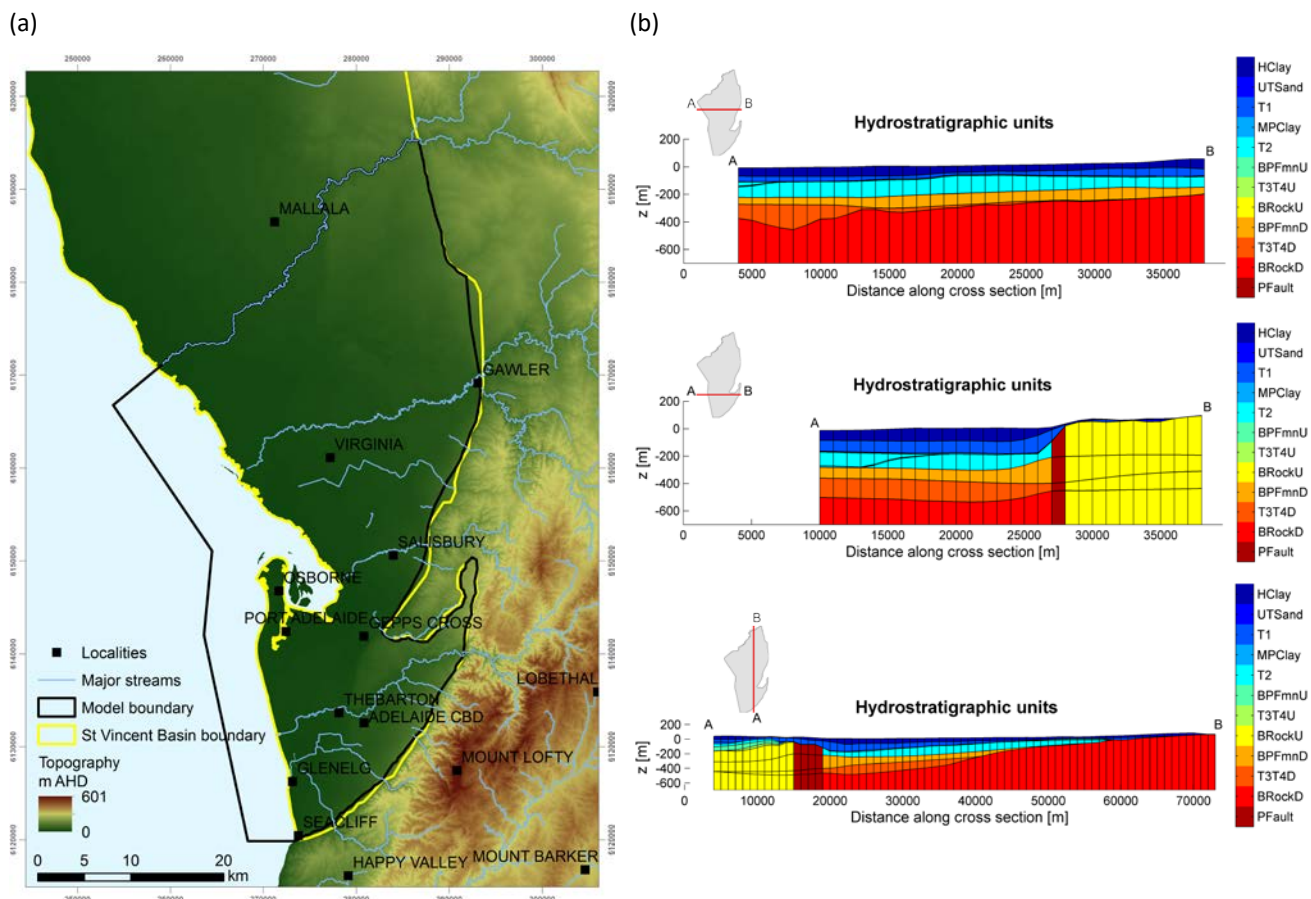


Figure 19 (a) Regional setting indicating the model extent and (b) selected cross-sections revealing the hydrostratigraphy as implemented in the model. The shorthand names for the zones are defined in Table 3

Table 3 Hydrostratigraphic units (zones of constant properties) and their abbreviation

ABBREVIATION	FULL NAME
HClay	Hindmarsh Clay aquitard
UTSand	Undifferentiated Tertiary Sand aquifer
T1	T1 aquifer
MPClay	Munno Para Clay aquitard
T2	T2 aquifer
BPFmnU	Blanche Point Formation upthrown of Para Fault (i.e., in the Golden Grove Embayment)
T3T4U	T3-T4 aquifer upthrown of Para Fault (i.e., in the Golden Grove Embayment)
BRockU	Bedrock upthrown of Para Fault (i.e., in the Golden Grove Embayment)
BPFmnD	Blanche Point Formation downthrown of Para Fault (i.e., in the Adelaide Sub-Basin)
T3T4D	T3-T4 aquifer downthrown of Para Fault (i.e., in the Adelaide Sub-Basin)
BRockD	Bedrock downthrown of Para Fault (i.e., in the Adelaide Sub-Basin)
PFault	Para Fault

7.2 Flow models (historical)

Three historical flow models were developed for calibration but also for the analysis of flow mechanisms under both pre-development and development conditions. They consist of:

1. A pre-development steady-state flow model (no pumping).
2. A pre-development transient flow model (May 1900 – April 1950, no pumping).
3. A development transient flow model (May 1950 – April 2013, pumping).

The steady-state model provides the initial heads for the pre-development transient model, which in turn provides conditions for the development transient model. The inflows and outflows considered in these models consist of:

- inflow from the MLR along the eastern/south-eastern boundary (hereafter referred to as eastern boundary for brevity), implemented using the general head boundary (GHB) package where the area of connection between boundary cells and the MLR was considered in the calculation of the conductance (Figure 20), and the head was based on topography;
- discharge towards the Gulf St Vincent, implemented using the GHB package (Figure 21);
- river-aquifer exchange along the streams and creeks within the model domain, implemented using the river (RIV) package and including seasonal variations (Figure 22a and Figure 22b);
- diffuse recharge across the top of the model domain, implemented using the recharge (RCH) package as a proportion of rainfall, the latter being both spatially (Figure 23a) and temporally variable;
- pumping (extraction/injection) in various aquifers, implemented using the well (WEL) package (Figure 23b and Figure 24).

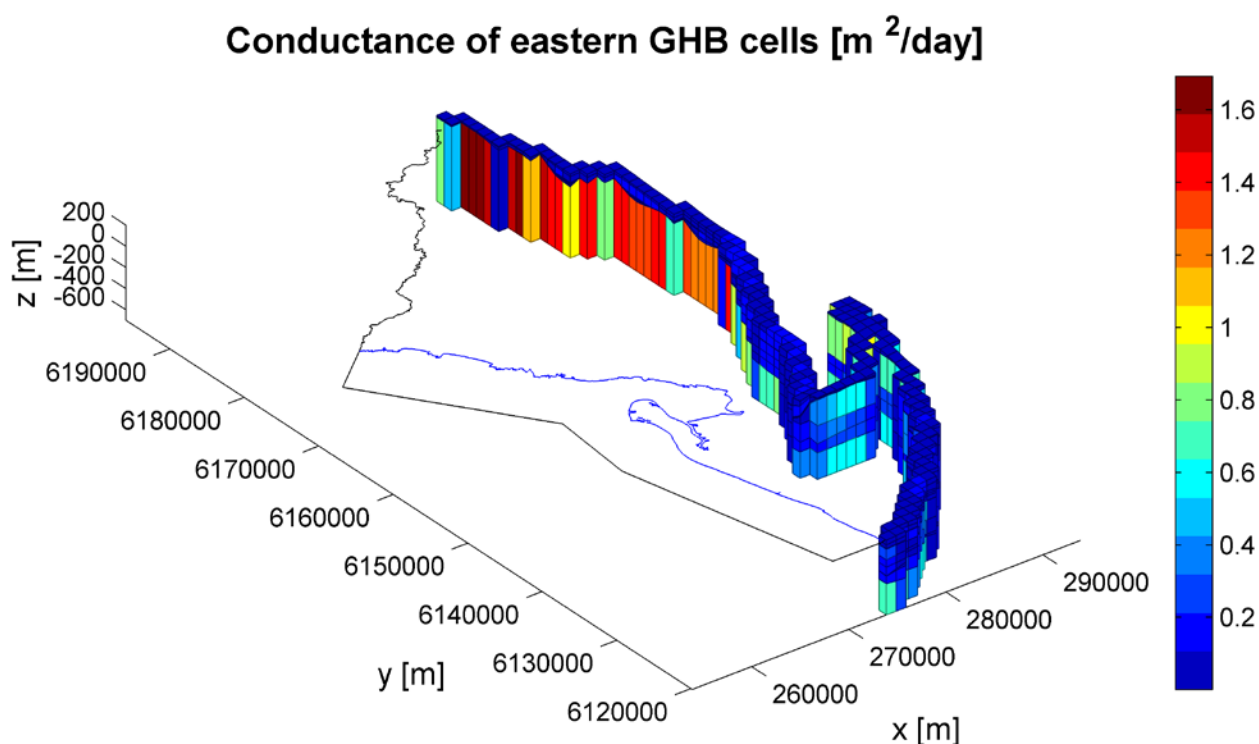


Figure 20 Conductance of the eastern GHB cells (3D view) when K equals the preferred value in all units. The distribution of values reflects differences in the area connecting the cells to the external source (product of the cell thickness by the length of boundary line crossing the cell)

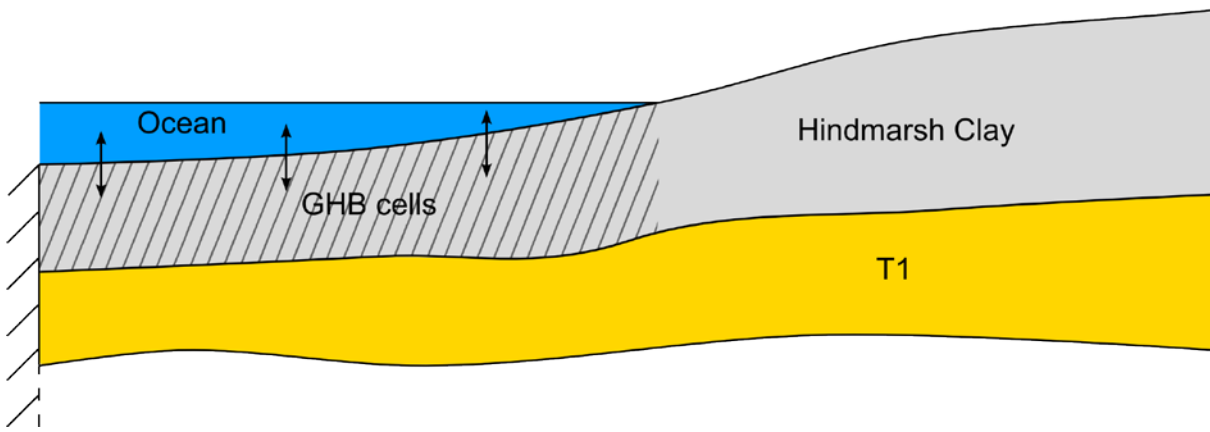
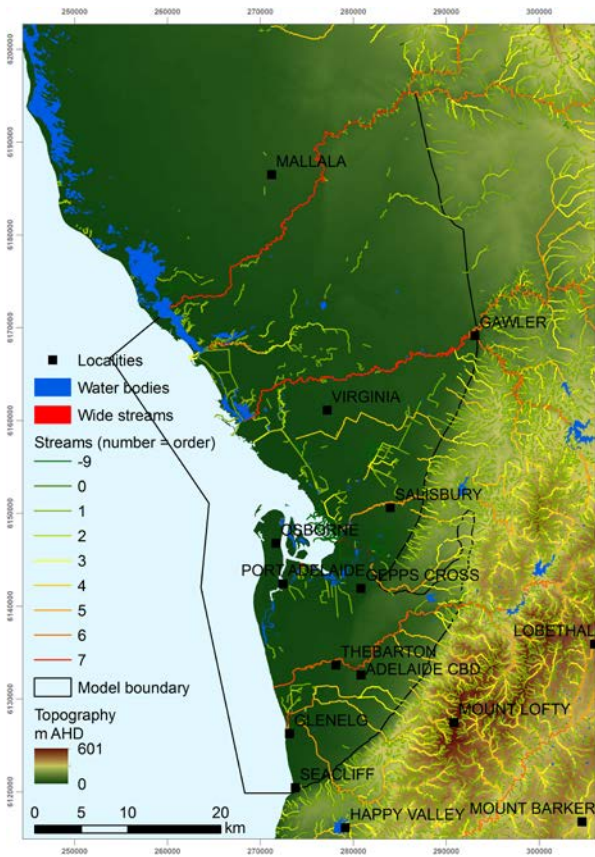


Figure 21 Conceptualization of the coastal boundary

(a)



(b)

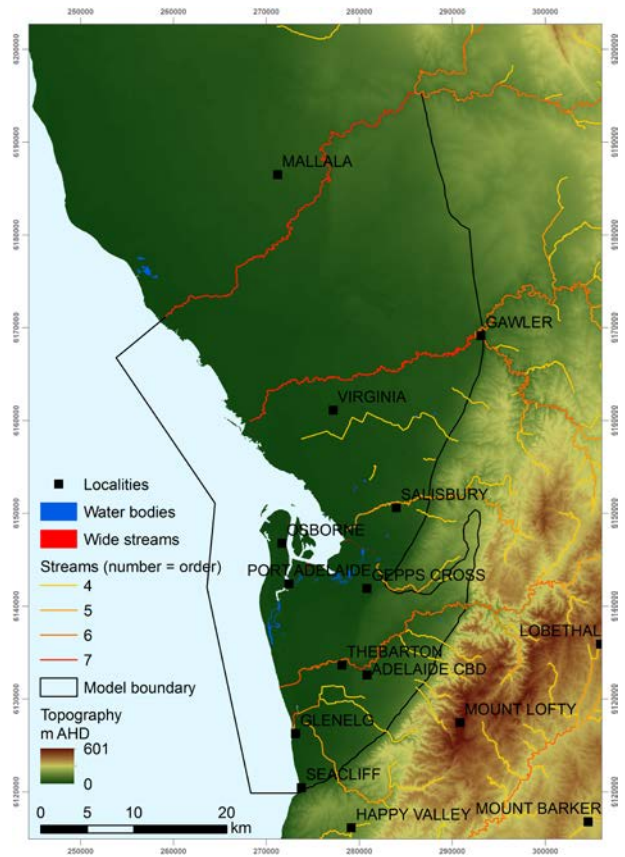


Figure 22 (a) All surface water features, considered in the winter months, and (b) perennial surface water features, considered in the summer months

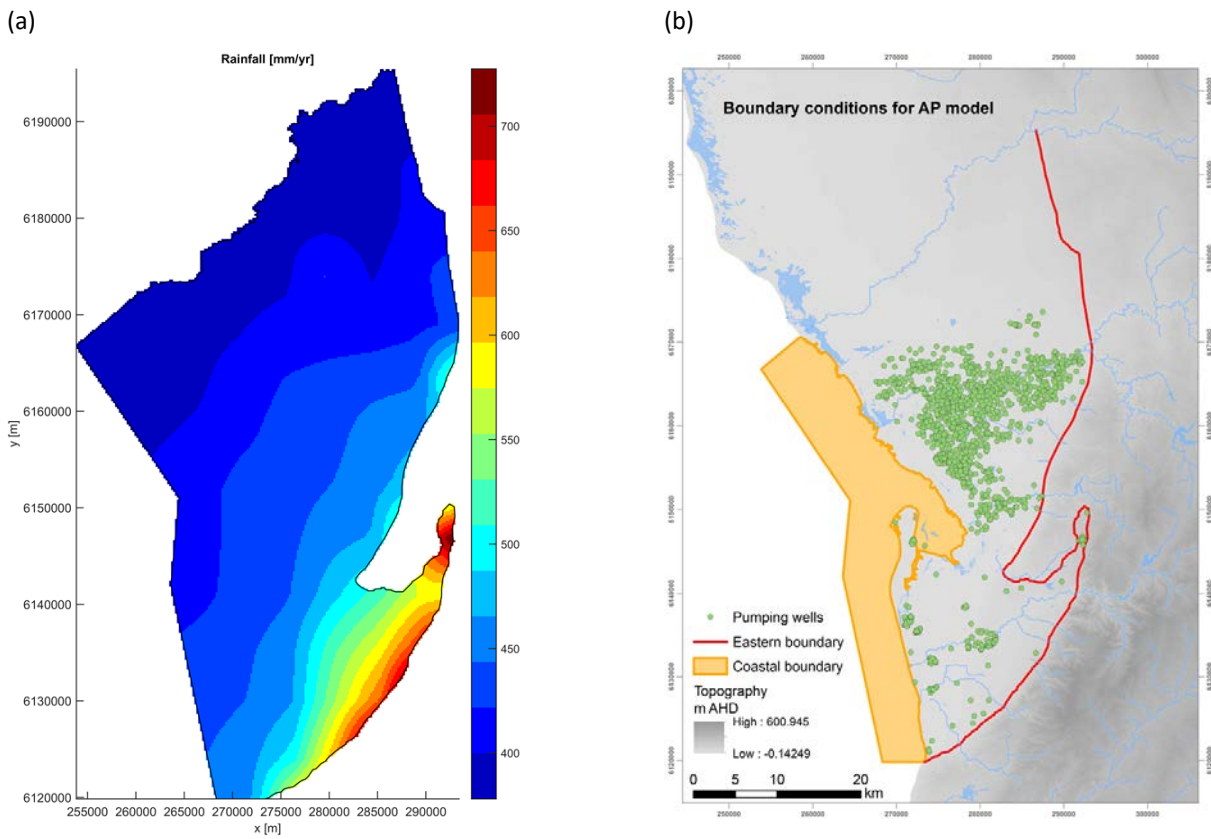


Figure 23 (a) Average annual rainfall distribution (1889–2013) and (b) location of pumping wells

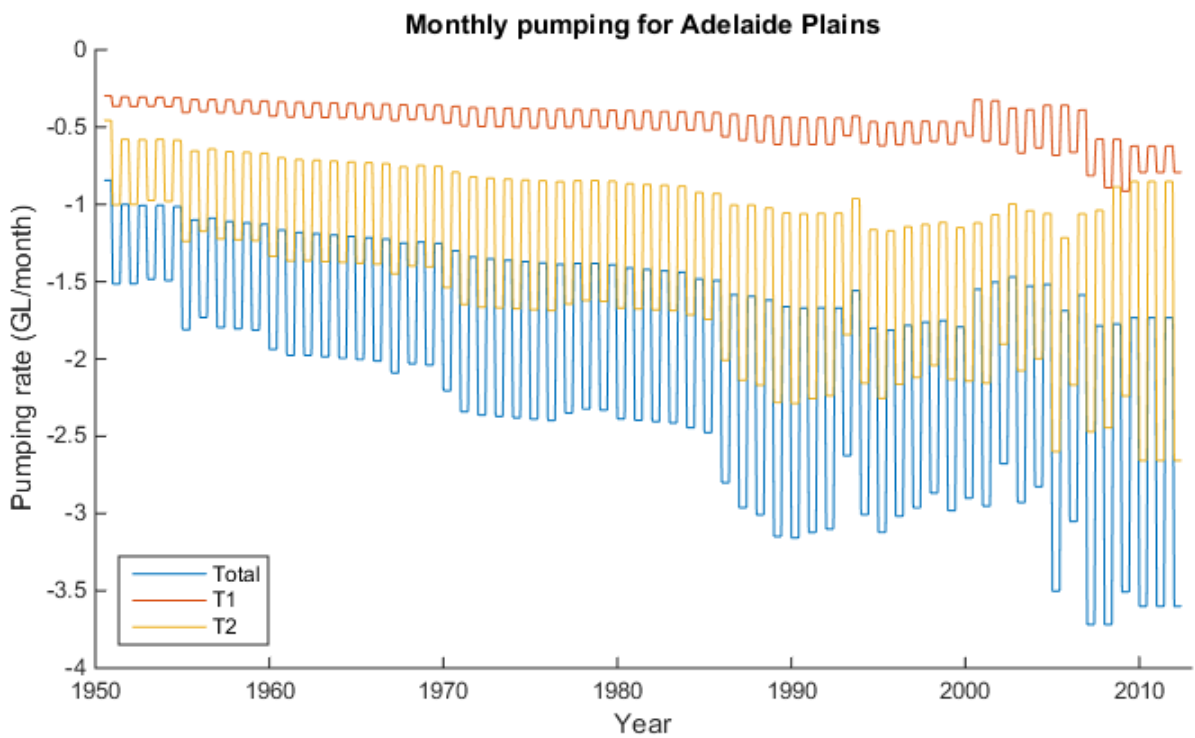


Figure 24 Monthly net pumping rates applied to the entire model domain, T1 and T2 aquifers

7.3 Flow models (future)

The aquifers of the Adelaide Plains provide a vital supply of groundwater to its many users and a suitable target for storage of captured stormwater following high surface flows. Efficient management of this resource necessitates a critical understanding of the impacts of changes to recharge and usage of the aquifers. Potential negative impacts to the aquifers form the focus of the scenario analyses, with emphasis on:

- Changes in rainfall due to a changing climate;
- Increased pumping by existing wells up to full allocations; and
- Increased usage of Managed Aquifer Recharge (MAR).

The investigation into the potential impacts described above was carried out through modification of the boundary conditions and stresses in the transient flow model as detailed in Table 4. The “base case” is the point of comparison for all other scenarios simulated. The base case used the monthly average of rainfall over the 10 years from 2002–2012 and applied this rainfall pattern for all future years until 2100, thus influencing the areal recharge as well as the eastern GHB head boundary. The pumping and MAR rates applied for the base case were the same as the 2012 year of the development period. These rates were repeated annually without change for the entire simulation. The coastal boundary remained unchanged.

Table 4 Summary of different scenarios applied including climate change, increased groundwater pumping and increased managed aquifer recharge

SCENARIO	EFFECT/DRIVER	IMPOSED BY	CHANGE SIMULATED	REFERRED TO AS
Base case	-	-	-	Base
Climate change	Reduced rainfall to the AP&MLR due to emissions	Reduced RCH and GHB	RCP4.5	RCP4.5
		Reduced RCH and GHB	RCP8.5	RCP8.5
Increased pumping	Increased demand	Increasing WEL pumping fluxes	+10%	Increased pumping
Decreased pumping	Decreased demand	Decreasing WEL pumping fluxes	-10%	Decreased pumping
Increased MAR	Increased demand	Increasing MAR schemes in WEL	Increased schemes (three-fold increase in total volume of MAR)	Increased MAR

7.4 Calibration

The model was calibrated using the automatic parameter estimation software PEST (Doherty 2013). Hydraulic head measurements were used for comparison with simulated heads of the historical groundwater flow models. More precisely, temporal mean values as well as deviations from the mean were used, as this strategy generally allows better estimation of hydraulic conductivity parameters on the one hand and of storage parameters on the other hand (Doherty *et al.* 2010; Knowling *et al.* 2015). Attempts were also made to constrain the calibration with Cl and ¹⁴C data conjointly to the transport models. Unfortunately, this strategy had to be abandoned because compatibility issues between MODFLOW-NWT and MT3DMS resulted in erratic behaviour during the PEST runs. Nevertheless, it was possible to run the transport models with the head-calibrated hydraulic parameters and preferred values for non-calibrated parameters (effective porosity and dispersivity), and to compare the outputs of these runs to the measurements.

A number of parameters deviated significantly from their preferred value during calibration. While some values can find reasonable justification, some others seem rather unlikely or would require further investigation to be deemed plausible. The most concerning of these (given their importance for the dynamics of the main aquifers) are the horizontal hydraulic conductivity in the T1 aquifer (0.63 m day⁻¹

when the preferred value from prior estimates was 9.4 m day^{-1}) and the specific storage in the T1 and T2 aquifers ($8.1\text{E-}07 \text{ m}^{-1}$ and $3.5\text{E-}06 \text{ m}^{-1}$ when the preferred value from prior estimates were $4.9\text{E-}04 \text{ m}^{-1}$ and $3.3\text{E-}04 \text{ m}^{-1}$, respectively).

The model performance statistics are given in Table 5. The SRMS for absolute hydraulic heads (2.99 %) is significantly smaller than in the previous modelling platform (6.77–7.79 % at given stress periods (Georgiou *et al.* 2011)). Nevertheless, a significant misfit ($SE > 1$) as well as a strong bias in weighted residuals can be observed for all the types of observations. The most likely reason for the misfit in mean hydraulic heads is the lack of intra-zone heterogeneity at least for hydraulic conductivity, while the most likely reason for the misfit in deviations from the mean head is a poor representation of inter-annual fluctuations in pumping. The misfit in Cl and ^{14}C has to be related to the fact that the model was not calibrated to Cl nor ^{14}C measurements, but also possibly to weaknesses in the parameterisation.

Table 5 Model performance statistics (definitions and keys for interpretation are given in Apx Table K.4)

STATISTIC	Mean hydraulic heads	Deviations from the mean hydraulic head	Absolute hydraulic heads ¹	Cl concentrations ¹	¹⁴ C activities ¹
RMS	9.11 m	3.22 m	8.46 m	929 mg L ⁻¹	27.9 pmC
SRMS	3.23 %	3.88 %	2.94 %	18.6 %	30 %
SE	6.09 (5.99–6.20)	6.11 (6.08–6.14)	15.35 (15.28–15.43)	6.45 (6.34–6.56)	55.9 (49.1–65.2)
MWR	0.32	0.00	4.09	4.04	29.9
R	0.95	0.54	0.94	0.08	0.42

1. Not part of the calibration dataset, but compared on the basis of the calibrated model

8 Water balance and its evolution

The regional water balance and its dynamics were quantified for pre-development, development and future periods on the basis of the new modelling platform. The results are presented in detail in Appendix K and summarised below with an emphasis on the water balance for the entire area as well as for the T1 and T2 aquifers individually. Given the limitations of the model (see below), it must be kept in mind that a large uncertainty surrounds these results. The description below is hence largely subject to verification and refinement in future works.

8.1 Pre-development (before 1950)

The pre-development model period is separated into a steady-state (long term behaviour up to 1900) and a transient model (1900 to 1950), and represents the long term average behaviour of the groundwater system prior to significant groundwater abstraction. Table 6 shows the decadal (1939–1949) average annual fluxes between the different zones at the end of the transient pre-development model. Flow occurs from one zone to another or across a model boundary. Because the flow direction changes spatially, both inflow and outflow can occur at the same time into or out of a single zone. For example, the Hindmarsh Clay both receives water from streams (3.28 GL yr^{-1}) but also discharges to them (2.49 GL yr^{-1}).

The model predicts that most of the inflows are from the streams (5.38 GL yr^{-1}), followed by lateral flow across the eastern boundary originating from the MLR (5.11 GL yr^{-1}) while the contribution from diffuse recharge is relatively small 0.66 GL yr^{-1} . Rainfall in the MLR provides lateral recharge to all zones but most prevalently into the Bedrock predominantly in the Golden Grove Embayment (3.37 GL yr^{-1}), followed by the T1 aquifer (0.55 GL yr^{-1}), the Hindmarsh Clay (0.32 GL yr^{-1}) and the T2 aquifer (0.30 GL yr^{-1}). Groundwater discharge occurs through the stream network (6.41 GL yr^{-1}) and the seafloor (5.81 GL yr^{-1}).

The table also illustrates the simulated flow dynamics and inter-aquifer exchanges in the Adelaide Plains. Groundwater flows upward from the Bedrock in the Golden Grove Embayment to the Undifferentiated Tertiary Sand aquifer (2.71 GL yr^{-1}), the T3T4 aquifer (1.51 GL yr^{-1}) and the T1 aquifer (0.74 GL yr^{-1}). Note that this significant groundwater pathway does not seem to have been recognised as such before. Hence, this constitutes a major difference between the current results and previous understanding and this warrants further investigation to confirm or deny this modelling outcome. Groundwater flows from the T3 and T4 aquifer into the Blanche Point Formation (0.84 GL yr^{-1}), and from the Blanche Point Formation to the T2 aquifer (1.32 GL yr^{-1}). There is a significant volumetric flux from the T2 aquifer to the T1 aquifer through the Munno Para Clay (2.88 GL yr^{-1}), despite of its relatively low vertical hydraulic conductivity (calibrated value: $1.4\text{E-}05 \text{ m day}^{-1}$). The T1 aquifer receives a significant amount of water from the Hindmarsh Clay (3.09 GL yr^{-1}), and discharges into it by about twice as much (6.62 GL yr^{-1}).

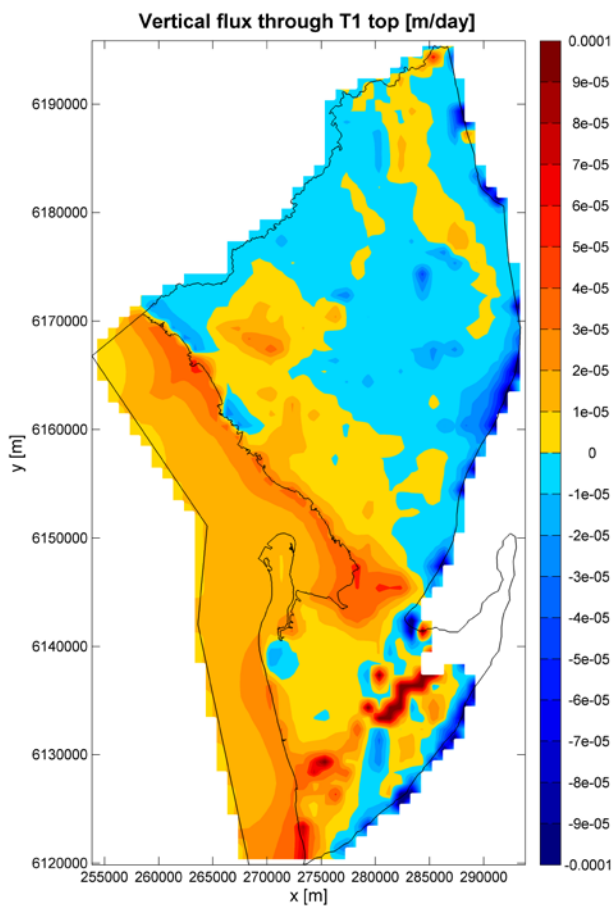
The spatial pattern of the vertical flux through the top of the T1 aquifer is shown in Figure 25a for the steady-state pre-development model. Positive values indicate upward flow and negative values indicate downward flows. It can be seen that the T1 aquifer generally gains water from the Hindmarsh Clay in the eastern part of the model domain, and then discharges into the Hindmarsh Clay further to the west especially along the coastline where the discharge intensity is high. Upward flow is also evident along the line of the Torrens River, as further illustrated in Figure 25b which shows groundwater-surface water exchange rates (here positive values indicate leakage from rivers, i.e. downward flow, and negative values indicate discharge to streams, i.e. upward flow).

Table 6 Decadal average annual fluxes (GL yr⁻¹) at the end of the transient pre-development model (1939–1949). Fluxes are from zones or boundaries indicated by the row names to other zones or boundaries indicated by the column names (except for the last row which indicates the change in storage in zones indicated by the column names). Values below 1x10⁻² are not shown. Colours are indicative of the magnitude, with blue to red colours highlighting small to large fluxes respectively as indicated in the lower table

	Hclay	UTSand	T1	MPClay	T2	BPFmnU	T3T4U	BedrockU	BPFmnD	T3T4D	BedrockD	Pfault	MLR	Streams	Coast	Recharge
Hclay		0.01	3.09											2.49	5.81	
UTSand			0.13					1.39						3.92		
T1	6.62	0.15		0.23	2.60			0.17		0.01		0.01				
MPClay			2.88		0.24											
T2		0.22	1.37	2.88		0.04				0.02						
BPFmnU					0.99		0.06	0.02								
T3T4U			0.75				0.68	0.15								
BedrockU		2.71	0.74				0.20	1.51								0.03
BPFmnD					0.33					0.02						
T3T4D			0.01							0.16						
BedrockD			0.02							0.01	0.02					
Pfault			0.01		0.07											
MLR	0.32	0.04	0.55	0.01	0.30	0.16	0.01	3.37	0.15	0.10	0.08	0.02				
Streams	3.28	2.10														
Coast																
Recharge	0.64	0.02														
Storage change	0.54	0.20	0.24				0.01	0.08		0.01		0.02				

Lower	Upper
0.001	0.1
0.1	2
2	4
4	6
6	>6

(a)



(b)

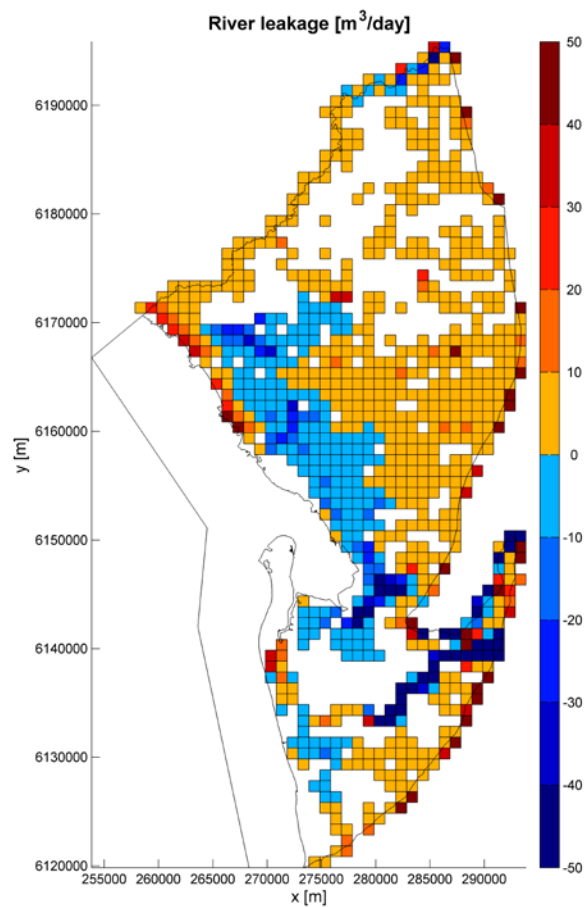


Figure 25 (a) Vertical flux through T1 top, and (b) groundwater-surface water exchange rates, both for the steady-state historical flow model

8.2 Development to present (1950–2013)

To investigate the impact of groundwater development on the aquifer system, the period of intense extraction between 1950 and 2013 was simulated using a transient flow model. The initial conditions are provided by the transient pre-development model (1900–1950). The simulated monthly and yearly water balance for the whole model as well as for the T1 and T2 aquifers are shown in Figure 26 and Figure 27.

A continual increase in pumping over time has occurred and it can be seen that this accounts for most of the seasonal dynamics of storage, with a lesser contribution from groundwater-surface water interaction. This results in a continually increasing storage loss from various units. The magnitude of the storage changes is much higher than that of the inflows across the model boundaries, meaning that these cannot supplement the water being abstracted. A slight but clear increase in inflow across the coastal boundary can be observed. An important internal redistribution of groundwater flow occurs across the zones, as revealed by the changes in flow dynamics of the T1 and T2 aquifers.

Figure 28 shows that the reduction in storage over this period is most significant in the Hindmarsh Clay and the T3-T4 aquifer. The decadal average annual flux (Table 7) further illustrates how the water is redistributed. The majority of the 32 GL yr⁻¹ of groundwater extraction occurs from the T1 (7.5 GL yr⁻¹) and T2 (20.27 GL yr⁻¹) aquifers. The T2 aquifer is pulling water in from above through the T1 aquifer directly (10.59 GL yr⁻¹) and through the Munno Para Clay (5.67 GL yr⁻¹). This water coming from the T1 aquifer ultimately originates from the Hindmarsh Clay, which loses 20.35 GL yr⁻¹ to the T1 aquifer. At its bottom the T2 is pulling significant amounts of water from the Blanche Point Formation (5.22 GL yr⁻¹). The Blanche Point Formation in turn is pulling water from the T3 and T4 aquifers (4.61 GL yr⁻¹).

It is noteworthy that even though most of the pumping occurs in the T1 and T2 aquifers, the change in storage for these zones is very small (Figure 26, Figure 27, and bottom row of Table 7). This is due to the fact that their specific storage values are low, resulting in large head decreases which drive inflow from surrounding zones. Storage in the Hindmarsh Clay and T3 and T4 aquifers is being depleted at an accelerating rate. As the groundwater extraction reduces the heads in the system, the streams turn from net gaining to net losing, which means the groundwater system is net gaining from the streams. The MLR contribution also increases as a consequence of the increasing gradient along the boundary, thus drawing more water into the system. Finally, the discharge to the coast is halved, and water starts flowing from the coast into the Hindmarsh Clay (0.40 GL yr⁻¹).

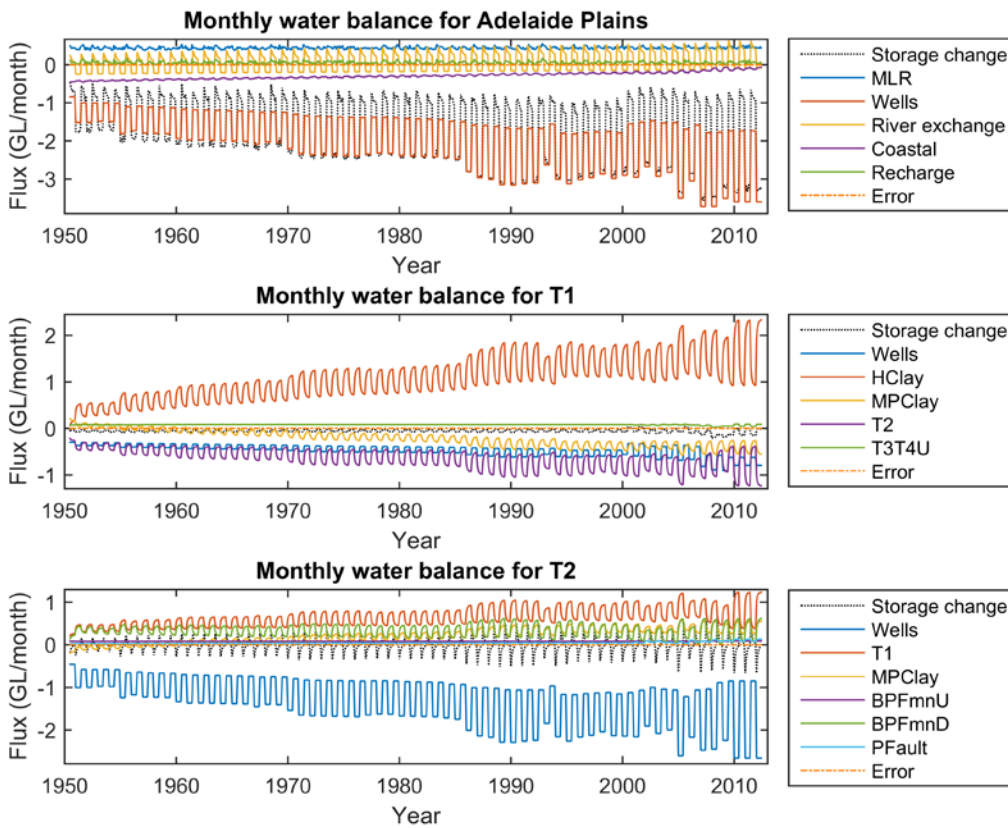


Figure 26 Monthly water balance for the transient development to present model (1950–2013) for the whole model and for the individual T1 and T2 aquifers. For clarity, only the units exchanging significantly with the T1 and T2 aquifers are shown

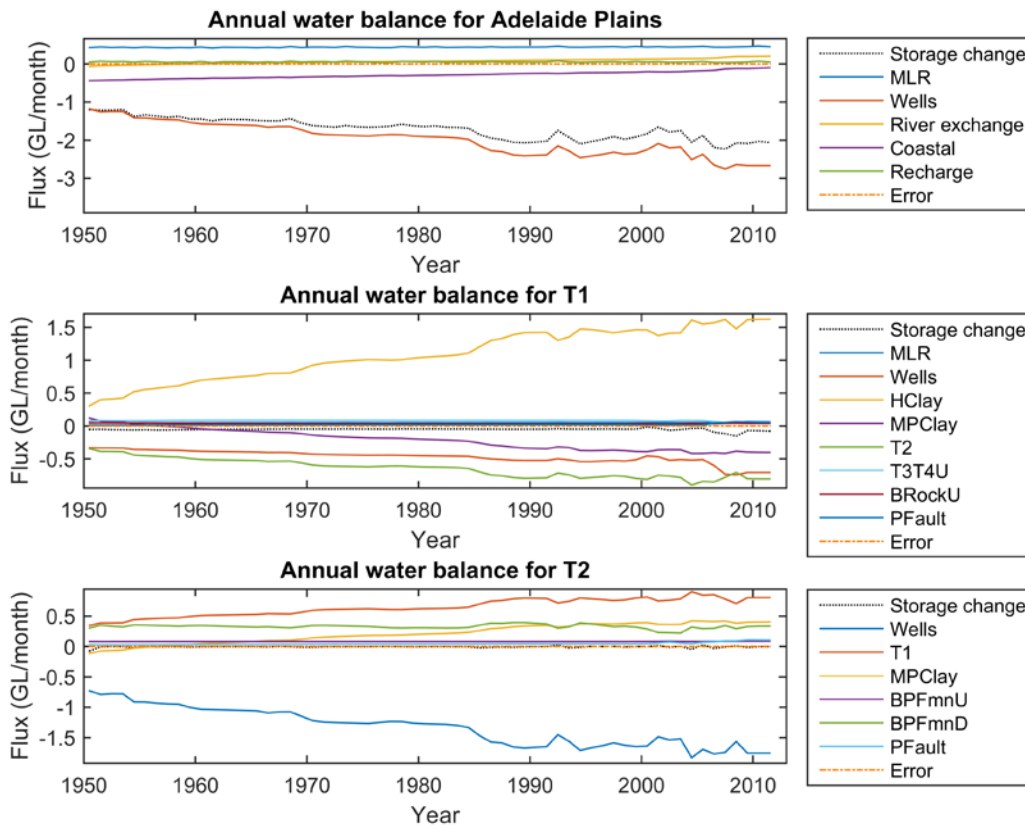


Figure 27 Yearly water balance for the transient development to present model (1950–2013) for the whole model and for the individual T1 and T2 aquifers. For clarity, only the units exchanging significantly with the T1 and T2 aquifers are shown

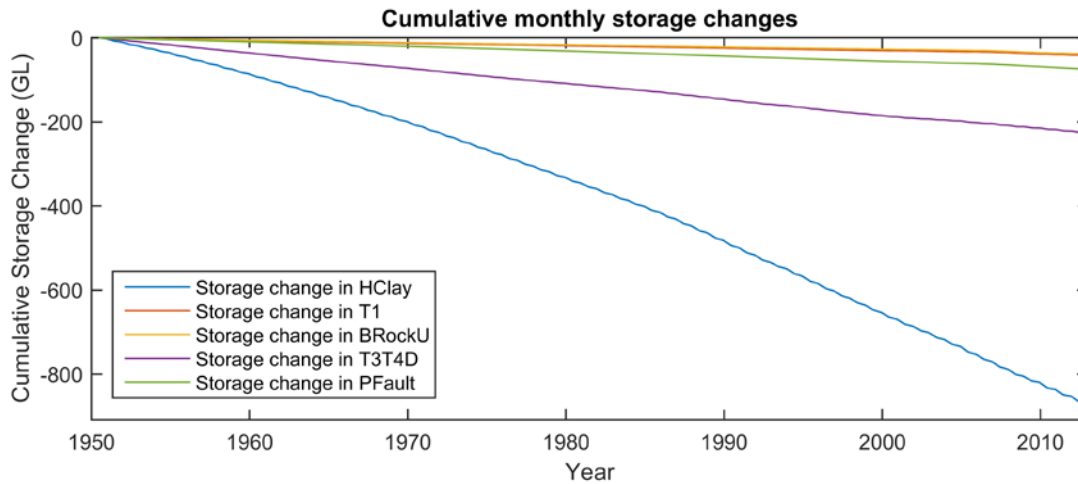


Figure 28 Cumulative change in storage (GL) for the development to present model (1950–2013) for units showing a significant storage change

Table 7 Decadal average annual fluxes (GL yr⁻¹) at the end of the transient development model (2002–2012). Reading keys are given in the caption of Table 6

	Hclay	UTSand	T1	MPClay	T2	BPFmnU	T3T4U	BedrockU	BPFmnD	T3T4D	BedrockD	Pfault	MLR	Wells	Streams	Coast	Recharge
Hclay			20.35											0.99	1.03	2.28	
UTSand			0.14					1.51								3.79	
T1	1.95	0.14		5.66	10.59		0.13	0.22		0.02		0.02			7.50		
MPClay			0.94		5.67												
T2		0.21	1.05	0.94		0.05			0.65								20.27
BPFmnU					1.07		0.07	0.03									
T3T4U			0.95				0.75	0.13							0.72		
BedrockU		2.57	0.65				0.19	2.21				0.03			0.68		
BPFmnD					4.15					0.58					0.02		
T3T4D			0.04						3.86								
BedrockD			0.02						0.03	0.06				0.03			
Pfault			0.47		0.98										0.16		
MLR	0.34	0.04	0.59		0.35	0.17		3.48	0.19	0.13	0.08	0.02					
Wells	0.02		0.05		0.26												
Streams	4.61	2.17															
Coast	0.40																
Recharge	0.56	0.02															
Storage change	-16.76	-0.28	-0.97		-0.10		-0.13	-0.97	-0.01	-3.10	-0.06	-1.54					

8.3 Future (2013–2100)

The results of the base case show strong similarity in behaviour to that of the system at the end of the development period. The cumulative change in storage in Figure 29 shows that the loss of storage to the system is quite large (850 GL yr⁻¹ by 2050 when summed across all zones) and that there is only a slow decrease in the absolute rate of change of storage over the years. The decadal flux matrix in 2050 (Table 8) is quite similar to that of the system over the 2002–2012 period (Table 7). Differences are partly driven by slightly different average pumping rates, as the pumping rates in the future scenarios are the repetition of a single year (2012). Higher inflows from the eastern, stream and coastal boundaries can also be observed, which compensate for the decrease in the storage loss rate.

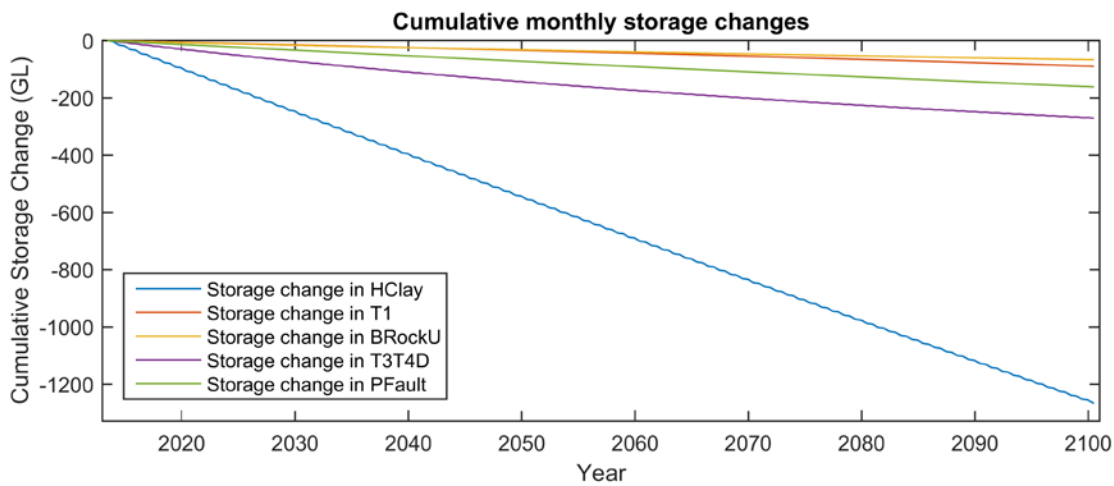


Figure 29 Cumulative changes in storage (GL) for the base case scenario (2013–2100) for units showing a significant storage change

Table 8 Decadal average annual fluxes (GL yr⁻¹) during the base case future model (2040–2050). Reading keys are given in the caption of Table 6

Yr 2050	Hclay	UTSand	T1	MPClay	TZ	BPFmnU	T3T4U	BedrockU	BPFmnD	T3T4D	BedrockD	Pfault	MLR	Wells	Streams	Coast	Recharge
Hclay			20.96											1.04	0.64	1.47	
UTSand			0.14					1.50							3.70		
T1	1.47	0.13		7.41	11.04		0.45	0.21		0.02				4.94			
MPClay			0.30		7.42												
T2		0.21	1.02	0.30		0.06			0.63					23.96			
BPFmnU					1.14		0.08	0.03									
T3T4U			0.45			0.80		0.17						1.72			
BedrockU		2.49	0.65			0.19	2.43					0.03		0.68			
BPFmnD					4.47					0.55							
T3T4D			0.03						4.13								
BedrockD			0.02						0.03	0.05			0.06				
Pfault			0.58		1.35									0.06			
MLR	0.37	0.04	0.64		0.39	0.18		3.79	0.22	0.15	0.13	0.03					
Wells	0.07				0.30												
Streams	5.22	2.19															
Coast	1.44																
Recharge	0.62	0.02															
Storage change	-3.68	0.26	0.95		0.07		0.16	0.78		3.39	0.04	1.93					

The effect of climate change when compared to the base case was seen to be insignificant in the future model scenarios with the differences in changes in storage of 0.2% and 0.3% for the RCP4.5 and RCP8.5 scenarios respectively. This is due to the ratio of diffuse recharge from rainfall to the total pumping being small in the model (<2%) across the base case and climate changes scenarios. The differences between the RCP4.5 and base case scenarios in the decadal average flux matrix in 2050 are also seen to be quite small (Table 9).

Table 9 Difference between base case and RCP4.5 scenarios in the decadal (2040–2050) average annual flux matrix (GL yr⁻¹). Values below 1x10⁻² are not shown

Yr 2050	Hclay	UTSand	T1	MPClay	T2	BPFmnU	T3T4U	BedrockU	BPFmnD	T3T4D	BedrockD	Pfault	MLR	Wells	Streams	Coast	Recharge
Hclay			0.06											0.00	-0.01	0.03	
UTSand			0.00					0.04							-0.04		
T1	-0.01	0.00		0.01	0.02		0.01	0.01		0.00				0.00			
MPClay			0.00		0.01												
T2		0.00	0.00	0.00		0.00			0.00					0.00			
BPFmnU					-0.01		0.00	0.00									
T3T4U			0.00			0.00		-0.01						0.00			
BedrockU		-0.06	-0.02			0.00	-0.02					0.00		0.00			
BPFmnD					-0.01					0.00							
T3T4D			0.00						0.00								
BedrockD			0.00						0.00	0.00							
Pfault			0.00		0.00									0.00			
MLR	-0.02	0.00	-0.03		-0.02	-0.01	-0.20	-0.01	-0.01	-0.04	0.00						
Wells	0.00				0.00												
Streams	-0.01	0.02															
Coast	-0.07																
Recharge	0.16	0.00															
Storage change	-0.02	-0.04	-0.03		0.00		-0.01	-0.06		-0.01	0.00	0.00					

Comparison of the cumulative storage change under future scenarios for changes in pumping and increased MAR demonstrate that the system has intuitive dynamics (Figure 30). More explicitly, increased pumping further increases storage loss, whereas decreased pumping or increased MAR reduces the storage loss compared to the base case. In all cases, a continued decrease in storage across can be observed, with similar consequences on groundwater circulations as described for the development period.

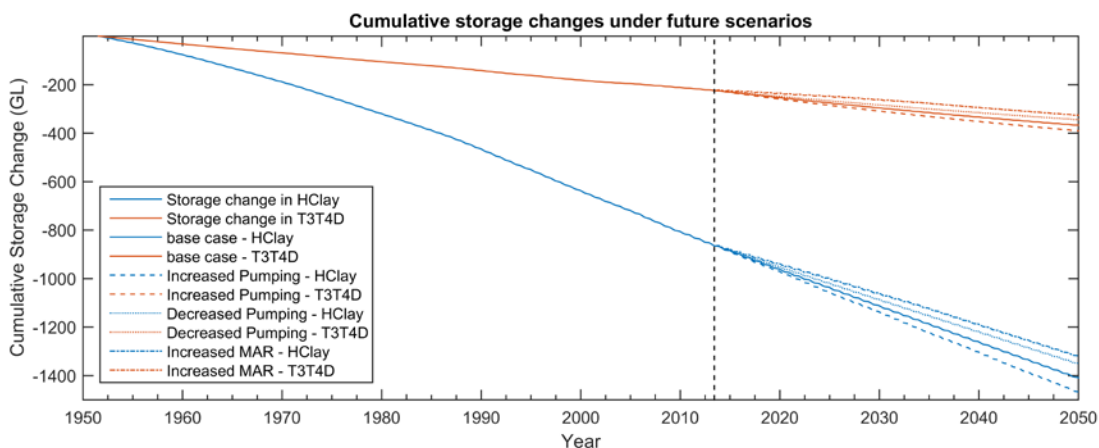


Figure 30 Comparison of cumulative storage change between base case, increased pumping, decreased pumping and increased MAR future scenarios (after the vertical dashed line which indicates the start of the year 2013) for units showing a significant storage change

9 Model capabilities and limitations

The current modelling platform is viewed as an ongoing effort towards achievement of regional-scale predictions of hydraulic heads, fluxes, Cl and ^{14}C . It should not be expected to provide locally accurate predictions. This is reflected in the calculated RMS which has been calculated for local observations of hydraulic heads, Cl and ^{14}C . On this basis, the local accuracy on modelled hydraulic heads, Cl and ^{14}C can be expected to be on average on the order of 8.60 m, 1410 mg L⁻¹ and 22 pmC, respectively. Unfortunately, local accuracy on flux predictions cannot be obtained in this way as no flux observations were used to compare with the model results.

The RMS only reflects the comparison of model results with local measurements. In contrast, the SRMS gives an idea of how well the model is capable of representing the variability of a given data type at the scale of the model, and is therefore a better measure of the suitability of the model to serve its purpose. The calculated SRMS for hydraulic heads, Cl concentrations and ^{14}C activities is 2.99 %, 28.28 % and 24.05 %, respectively. In view of these and assuming that the variability of a given data type is dominated by regional-scale variability (as opposed to local-scale variability), the model could be deemed suitable for regional-scale prediction of hydraulic head but not for Cl and ^{14}C .

The suitability of the current model to predict groundwater fluxes is difficult to assess as no flux observations were used to compare with the model results. Parameter uncertainty analysis could give some hints on the uncertainty surrounding flux estimates but a reliable estimation of uncertainty cannot be achieved solely on this basis. Predictive uncertainty on flux estimates using the current model could be performed as a next step, but this still would not capture the uncertainty induced by potential structural/conceptual errors (such as the absence of intra-zone heterogeneity or the coarse grid resolution). The lack of capacity to estimate uncertainty on flux predictions is considered to be a major limitation of the current model.

A number of results in this study indicate that the current model might contain significant structural/conceptual errors which could compromise the capacity of the model to provide reliable future predictions (with mostly unknown consequences which will be prediction-dependent):

- The influence of grid resolution on the simulation results is indicative of structural error. This was shown to affect not only groundwater-surface water interactions but also the flow across the MLR boundary.
- The initial condition was shown to influence the results as a dynamic equilibrium is not reached at the end of the pre-development period. This may bias the results, although this bias is insignificant for the development period as pumping effects largely surpass this artefact.
- A number of parameters deviated significantly from their preferred value during calibration. While some values can find reasonable justification, some others seem rather unlikely or would require further investigation to be deemed plausible. The most concerning of these (given their importance for the dynamics of the main aquifers) are K_H in the T1 aquifer and S_S in the T1 and T2 aquifers.
- Strong biases are observed in the weighted residuals of the calibration dataset. These generally indicate that both the spatial and temporal variability are underestimated by the model, and also that some areas have a systematic bias towards either low or high values.

Key recommendations for future improvements of the modelling platform are listed in Appendix K.

Part III Synthesis

10 Comparison of approaches and ways forward

10.1 Diffuse groundwater recharge

Calibration of the regional flow model to heads suggests that the value for diffuse groundwater recharge is 0.08 % of rainfall, i.e., an order of magnitude smaller than the value inferred from the CMB method (0.8 % of rainfall). There are reasons for the CMB-based estimate to be an overestimation of the diffuse recharge (see section 3.2). Nevertheless, the recharge parameter in the regional flow model reached its lower bound during calibration, meaning that it could have been smaller if the bounds were taken wider. This could be seen as an indication of structural model error. Namely, there are a large number of domestic (non-licensed) wells in the Quaternary aquifers that were not included in the model. Individual pumping rates from these wells are relatively small, but together they were estimated to sum up to about 2 GL yr⁻¹ for the sedimentary aquifers (Martin 2011). Groundwater levels would in reality be affected by these wells, and consequently it is possible that a small calibrated recharge stems from a compensation of the lack of inclusion of these wells in the model. Observed misfits between measured and simulated Cl and ¹⁴C suggest that diffuse recharge in the model could be too small.

A number of the issues associated with the application of the CMB should be overcome using a regional Cl transport model coupled to the regional flow model and calibrating recharge not only to hydraulic head data, but also to Cl concentration data. In contrast with the classical CMB, the mixing of waters of different origins (diffuse recharge, river leakage, MLR) would be fully accounted for, as mixing is integral part of the transport model. While this strategy was attempted during the course of the project, it finally had to be abandoned due to compatibility issues between MODFLOW-NWT and MT3DMS. The approach is nevertheless promising and should eventually provide more reliable estimates of diffuse recharge.

10.2 Groundwater-surface water interaction

River leakage in the region is estimated to be at least 4.7 GL yr⁻¹ in 2014–2015 based on a differential stream gauging approach. Based on the regional model calibrated to heads, river leakage is estimated to be 6.78 GL yr⁻¹ under development conditions (2002–2012 average), respectively. While both methodologies are prone to significant uncertainties, the relatively good agreement between such independent approaches suggests that the range of values obtained is robust.

The direct measurements can be expected to be more accurate than the modelling results at the points in space and time at which they were taken. However, globally the modelling results are expected to be more robust as they integrate a number of regional and temporal constraints implied by: the geological and hydrogeological setting; ungauged surface water features; variations in stresses (climate, pumping); hydraulic heads; and the regional water balance. In addition, the model allows investigation of past and future exchange rates, whereas the direct measurements only allow characterisation of the present.

In order to make the most of both approaches, the direct measurements should be included in the calibration dataset of the regional model. Given the apparent significance of groundwater-surface water interactions in the water balance (e.g. Table 6) this approach is worth pursuing in combination of improving the spatiotemporal characterisation of groundwater-surface water exchanges. Specifically, measurements should aim to quantify both intra and inter-annual fluctuations of the exchange rates and should target surface water features that are poorly documented so far such as Dry Creek, Cobbler Creek, Smith Creek, Light River, lakes and farm dams. The status (perennial/ephemeral), geometry (width) and elevation of rivers should also be better documented.

10.3 Flow across the faults

The total flow across the faults (i.e., across both Para Fault and Eden-Burnside Fault) from the MLR to the Plains is estimated to be 2 – 4 GL yr⁻¹ based on a simple ¹⁴C cross-sectional model along a transect of the NAP (section 5.2). In comparison, the total flow across the faults predicted by the steady-state historical regional flow model is 5.36 GL yr⁻¹. While both methodologies are prone to significant uncertainties, the close agreement between such independent approaches suggests that the range of values obtained is robust.

The estimate based on the simple ¹⁴C cross-sectional model is likely to be prone to major uncertainty as the ¹⁴C values might not be representative of current flow conditions and it ignores the spatial variability of flow rates along the faults (see section 5.2). It might nevertheless be worth including this estimate as a calibration target of the regional model, in which case the flow rate could be compared at the point where the transect meets with the fault, thus removing the uncertainty related to the upscaling.

A number of simplifying assumptions associated with the simple ¹⁴C cross-sectional model are removed when using a regional ¹⁴C transport model coupled to the regional flow model and including directly the ¹⁴C measurements in the calibration dataset. As already mentioned before for Cl transport, the mixing of waters of different origins (diffuse recharge, river leakage, MLR) would be fully accounted for. In that case, there would be no need for including the estimate from the simple cross-sectional model as a calibration target, because this information would be superseded by the use of the regional ¹⁴C transport model. This strategy was attempted but unfortunately, for the same reason as for Cl transport it had to be abandoned. The approach is nevertheless promising and should eventually provide more reliable estimates of flow across the faults, and more generally of velocities in the regional flow model.

10.4 Leakage through the Munno Para Clay

Two core-based estimates of vertical hydraulic conductivity were derived and used conjointly with a year 2014 head-gradient map between the T1 and T2 aquifers to estimate current leakage through the Munno Para Clay at regional scale (section 6.2). This resulted in an upward leakage of 0.36 GL yr⁻¹ in the CAP and a downward leakage of 1.19 GL yr⁻¹ in the NAP. In contrast, an average total upward leakage of 0.94 GL yr⁻¹ and downward leakage of 5.67 GL yr⁻¹ for the past 10 years was obtained using the regional flow model. These differences can be mostly attributed to the 4 times larger vertical hydraulic conductivity used in the model (1.5E-05 m day⁻¹) than found in Appendix E (3.4E-06 m day⁻¹). This difference in hydraulic conductivity could easily be explained by the fact that core-based estimates are not likely to be representative of the regional scale hydraulic conductivity.

11 Revised groundwater flow mechanisms

The investigations conducted in this project suggest some revision of the groundwater flow mechanisms to the Tertiary aquifers of the Adelaide Plains. It must be kept in mind that a large uncertainty commensurate to the limitations of the model surrounds these conclusions. The new understanding is hence subject to verification and refinement in future works.

Schematically, early investigations suggested that the inflows to the Tertiary aquifers were dominated by river leakage flow downward through the Quaternary aquifers (Miles, 1952; Shepherd 1975), while later investigations suggested that the inflows to the Tertiary aquifers were dominated by lateral flow from the MLR (Gerges, 1999, 2006). The results of this study suggest that both mechanisms (river leakage and lateral flow) contribute significantly to the inflows to the Tertiary aquifers under pre-development conditions. This conclusion is in line with the findings of Green *et al.* (2010).

On the basis of the regional groundwater flow model calibrated to heads, under pre-development conditions the downward flux from the Quaternary sediments into the T1 aquifer is estimated to be 3.09 GL yr⁻¹ (Table 6). Of this, a maximum of 0.32 GL yr⁻¹ originates from the MLR via lateral flow into the Quaternary sediments, i.e., at least 2.77 GL yr⁻¹ (the remaining part) originates from vertical recharge in the Plains (mostly from river leakage as diffuse recharge is 10 times less than river leakage). On the other hand, the total lateral flux from the MLR into the Plains is estimated to be 5.11 GL yr⁻¹. Of this, 0.32 GL yr⁻¹ flow into the Quaternary sediments whereas 0.55 and 0.30 GL yr⁻¹ flow directly into the T1 and T2 aquifers, respectively. The remaining part is principally lateral flow into the Bedrock in the Golden Grove Embayment (3.37 GL yr⁻¹) and this subsequently feeds the Tertiary aquifers by upward flow in that area. The latter groundwater pathway is significant and does not seem to have been recognised as such before. Hence, this constitutes a major difference between the current results and previous understanding and this warrants further investigation to confirm or deny this modelling outcome, including new data analysis and field work as little data is available in the deep aquifers of the Golden Grove Embayment.

The simulation results show clear changes between the past, present, and future conditions of the groundwater system (Figure 31). Prior to pumping, the inflows and outflows to the system were well balanced. Introduction of pumping changed this balance and caused significant storage depletion, which amounts to 64 % of the inflows to the system for the year 2012. The low specific storage of both the T1 and T2 aquifers implies that increased pumping draws the head down in these aquifers without the capacity to release large quantities of water. This induces large head gradients between the T1 and T2 aquifers and units above and below. In response, the Quaternary sediments provide the largest amounts of water via release of storage. Water also originates from the underlying T3 and T4 aquifers. In a business-as-usual predictive scenario, storage loss continues into the future, but at a decreasing rate as other sources start to contribute more water. Stream infiltration and inflow from the MLR contribute slightly more to the system, but the largest effect is from the flow across the coastal boundary, which switches from net outflow to net inflow.

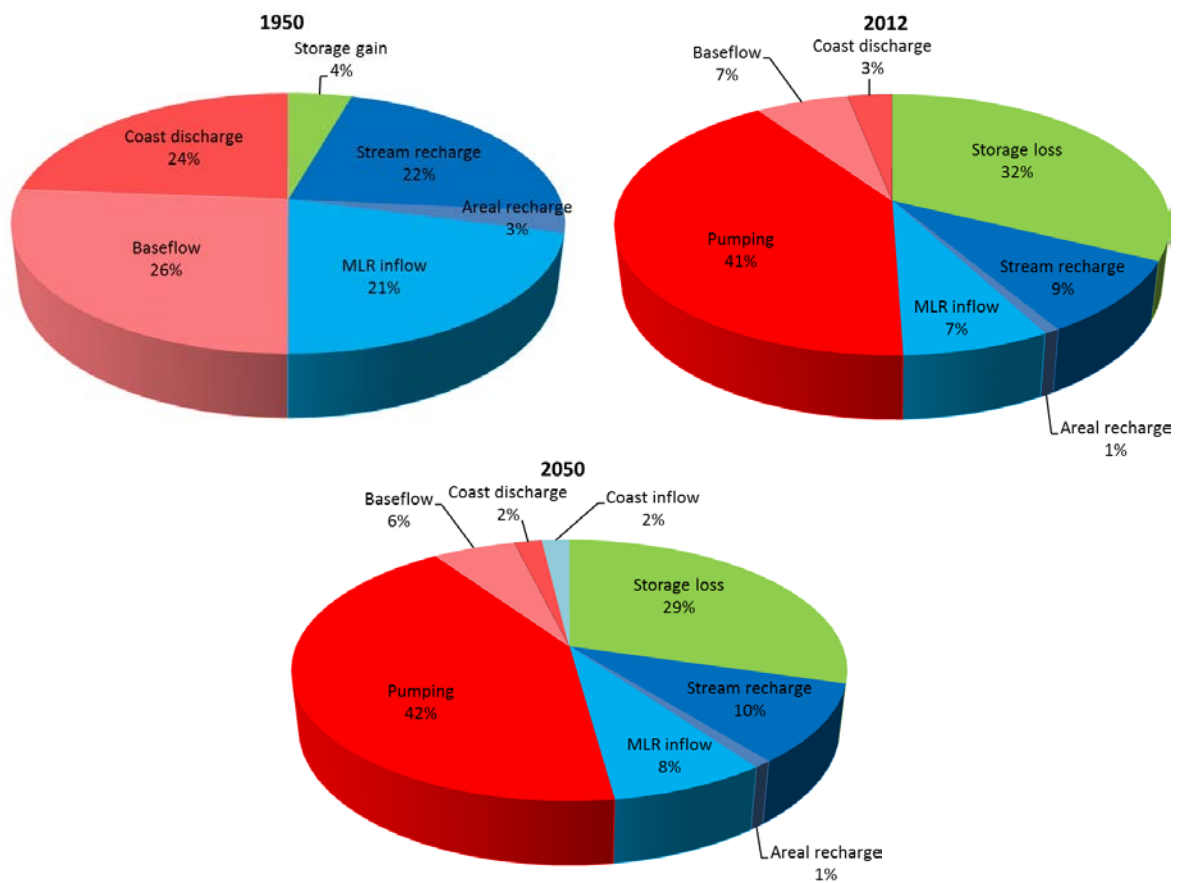


Figure 31 Decadal average water balance components as a percentage of the total balance for pre-development (in 1950), development (in 2012) and future (base-case in 2050) periods. Red coloured pieces of the pie indicate flow out of the system, blue pieces indicate flow into the system, and green indicates storage changes (either gain or loss)

The conceptual model of the Adelaide Plains groundwater system under current conditions is depicted graphically in Figure 32. This figure reflects the current understanding which is based on previous studies complemented by the results of the present studies that have improved and further refined the existing model. The system is currently in a stressed state, mainly as a result of pumping from the Tertiary aquifers. This has led to a strong decline of groundwater levels over the past decades and extensive cones of depression have formed around the main areas of pumping (Figure 9 and Figure 10). In large parts of the system, flow directions have been reversed compared to the pre-development conditions, which is supported in this study by the analysis of ⁴He in the pore water of the Munno-Para aquitard as well as by the model results.

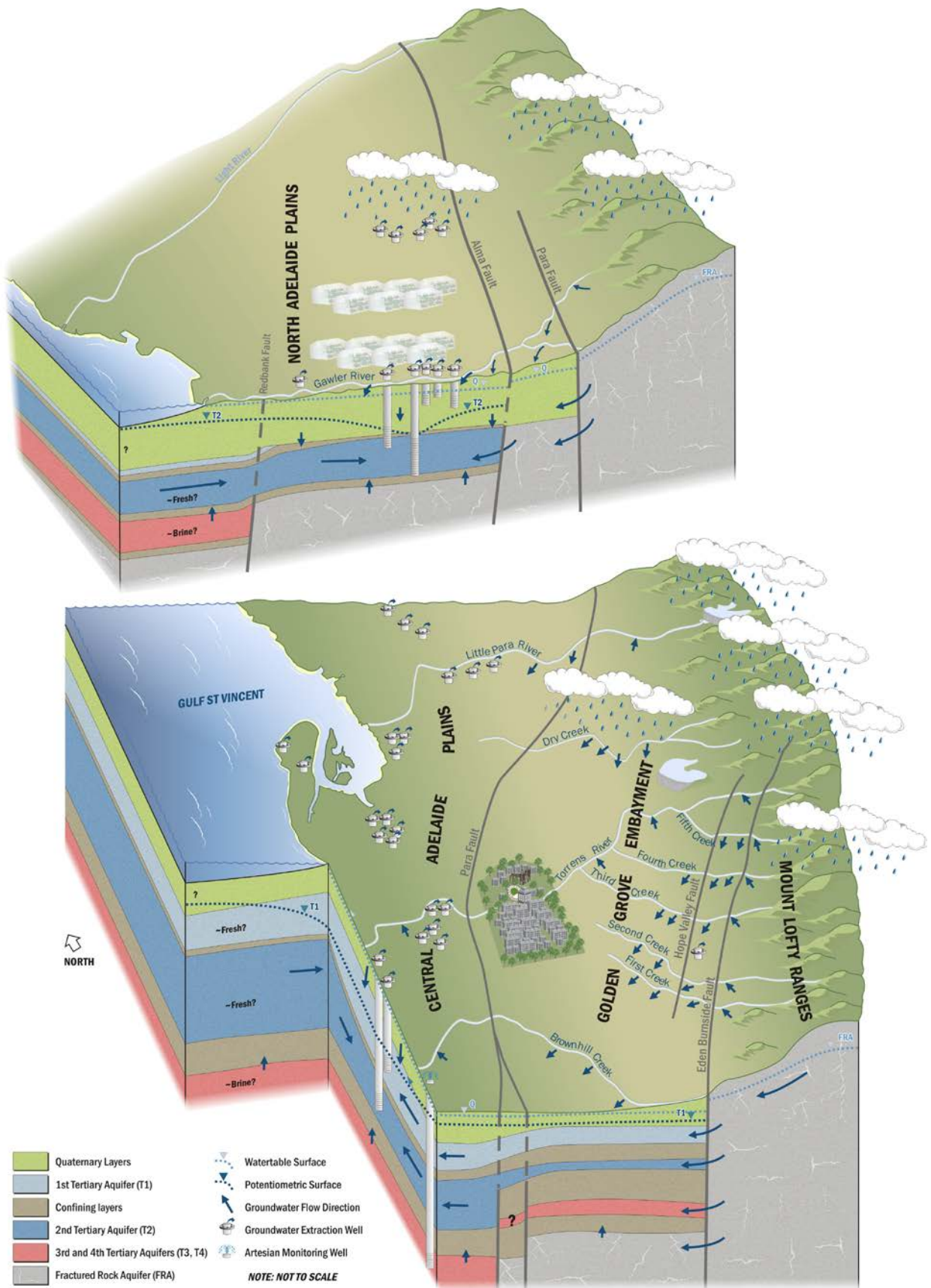


Figure 32 Hydrogeological conceptual model of the Adelaide Plains groundwater resources

12 Implications for groundwater resources management

The impacts of groundwater abstraction raise a number of key management questions. The observed widespread decline of potentiometric levels indicates that total pumping is presently occurring at a rate that largely exceeds natural inflows. The modelling results suggest that the total inflow to the aquifers is no more than in the order of 10 – 15 GL yr⁻¹. Data on groundwater pumping provided by Georgiou *et al.* (2011) indicate a total annual extraction in the order of 30 GL yr⁻¹ in recent years, suggesting that pumping exceeds the natural inflows by a factor 2 to 3. According to the model results, this implies a strong decline in storage in the groundwater system and increased cross-formational flow.

The regional groundwater flow model has been used to study how the groundwater flow circulations are modified in response to pumping. Despite the fact that abstraction is largest from the T1 and T2 aquifers, the model results suggest that most of the storage depletion occurs in the Hindmarsh Clay (the name of the zone in the model lumping together the Quaternary sediments). Given the relatively high groundwater salinity found in the Quaternary sediments, this implies significant risks of increase in salinity in the Tertiary aquifers. However, the time frame over which this might become an issue for groundwater usage remains unknown, and there is currently limited evidence of increased salinity in the upper Tertiary aquifer in response to this.

The model results further suggest that more groundwater is flowing vertically upward from the Bedrock and the T3 and T4 aquifers into the overlying Tertiary aquifers to compensate the loss of groundwater by pumping. However, this needs to be verified with targeted monitoring of the Tertiary aquifers and in relation to the deeper units, including examination of any observational evidence of upward flow of saline water from the T3/T4 aquifers into the overlying Tertiary aquifers. A detailed study of the seawater interface in the Willunga Embayment showed that besides seawater, old (> ~20,000 years) hypersaline groundwater exists. Such hypersaline groundwater was also identified in observation wells across the Adelaide Plains, in particular in the T3/T4 and fractured rock aquifers. The upward flow from these units towards the T1 and T2 suggests that salinization from deep-seated sources might become more prevalent. This risk cannot be fully assessed until the distribution of the hypersaline groundwater is better understood.

Groundwater seems to have started to flow inland from the coast, which is apparent from the measured hydraulic heads (Figure 9 and Figure 10) and is suggested by the results of the model. However the location of the salt water interface in the deeper confined aquifers is unknown and it may be located some distance off-shore. The adequacy of the current monitoring network to provide early warning of any intrusion of salt water along the coast should be assessed, and further modelling including testing different coastal boundary conceptualisations appears necessary.

In response to the abstraction, river leakage has also increased substantially according to the model. While further work is warranted to confirm this result, this suggests the need for managing groundwater and surface water conjunctively, and also points towards potential adverse effects of pumping on river/wetland ecosystems.

The modelling of future scenarios suggests that the storage depletion will be ongoing and therefore that the adverse effects depicted above will be intensified. If this result is confirmed, further development of managed aquifer recharge (MAR) might be required to curb the ongoing declining trend if the present day pumping allocations are to be maintained.

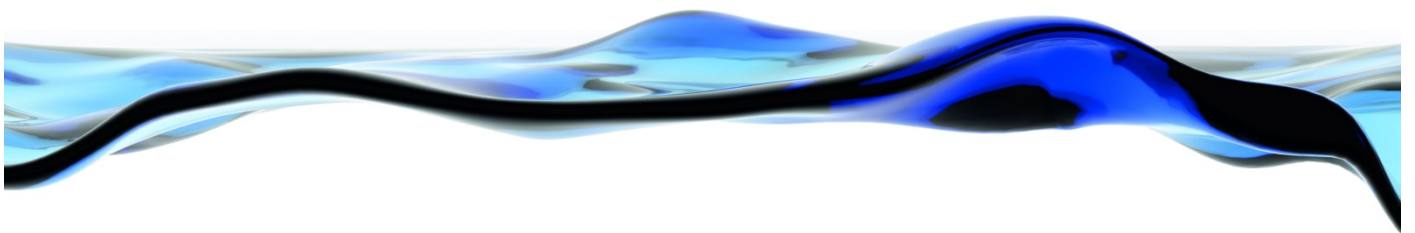
13 Recommendations

The regional groundwater flow and transport modelling platform is believed to be the best tool possible to integrate the data as it allows accounting for all constraints implied by the regional setting. It is also the only tool available to investigate future scenarios on a physical basis. However, even though a number of steps were undertaken in this project to improve the model, some key issues have been identified and call for further work before the model could be deemed suitable for making reliable future predictions including rigorous uncertainty quantification. The key recommendations for further improvement listed in Appendix K point towards a number of data gaps and modelling tasks. It is recommended that these steps be undertaken in order to achieve a better tool to understand the Adelaide Plains groundwater system and to inform decision makers regarding water management questions.

14 References

- Baird DJ (2010) Groundwater recharge and flow mechanisms in a perturbed, buried aquifer system: Northern Adelaide Plains, South Australia. Flinders University.
- Cranswick RH, Cook PG (2015) Scales and magnitude of hyporheic, river–aquifer and bank storage exchange fluxes. *Hydrological Processes*, n/a-n/a.
- Currie D, Braithwaite H, McCallum C (2011) 'Adelaide Plains Groundwater Investigation Projects part 3: Surface water / groundwater interactions.' Sinclair Knight Merz, Adelaide, South Australia.
- Doherty J (2013) 'Manual and Addendum for PEST: Model-Independent Parameter Estimation.' (Watermark Numerical Computing: Brisbane, Australia)
- Doherty J, Hunt RJ (2010) 'Approaches to highly parameterized inversion—A guide to using PEST for groundwater-model calibration.' U.S.G.S., Report 2010–5169.
- Georgiou J, Stadter M, Purczel C (2011) 'Adelaide Plains groundwater flow and solute transport model.'
- Gerges NZ (1999) The Geology and Hydrogeology of the Adelaide Metropolitan Area Volume 1 & Volume 2. PhD thesis, Flinders University.
- Gerges NZ (2001) 'Northern Adelaide Plains groundwater review.' Department for Water Resources, DWR Report 2001/013, Adelaide.
- Gerges NZ (2006) 'Overview of the hydrogeology of the Adelaide metropolitan area.' Department of Water, Land and Biodiversity Conservation, DWLBC Report 2006/10, South Australia.
- Green G, Watt E, Alcoe D, Costar A, Mortimer L (2010) 'Groundwater flow across regional scale faults.' Government of South Australia, through Department for Water, DFW Technical Report 2010/15, Adelaide.
- Hodgkin T (2004) 'Aquifer Storage Capacities of the Adelaide Region.' DWLBC, Report no 2004/47.
- Hutton RG (1977) 'Northern Adelaide Plains surface Water assessment 1971-1975.' Department of Mines, Adelaide, South Australia.
- Knowing MJ, Werner AD, Herckenrath D (2015) Quantifying climate and pumping contributions to aquifer depletion using a highly parameterised groundwater model: Uley South Basin (South Australia). *Journal of Hydrology* 523, 515-530.
- Leaf AT, Hart DJ, Bahr JM (2012) Active Thermal Tracer Tests for Improved Hydrostratigraphic Characterization. *Ground Water* 50, 726-735.
- Manning AH, Clark JF, Diaz SH, Rademacher LK, Earman S, Niel Plummer L (2012) Evolution of groundwater age in a mountain watershed over a period of thirteen years. *Journal of Hydrology* 460–461, 13-28.
- Martin R (2011) 'Estimating Non-Licensed Groundwater Use Across the Adelaide Plains PWA.' Australian Groundwater Technologies, Report no 1079-10-AAA.
- Miles KR (1952) 'Geology and underground water resources of the Adelaide Plains area.' (Department of Mines: Adelaide)
- REM (2006a) 'Tertiary Aquifers of the Adelaide Coastal Plains Groundwater Model: Steady-state Model Set-up and Calibration Report.' Resources and Environmental Management, Adelaide, South Australia.
- REM (2006b) 'Tertiary Aquifers of the Adelaide Coastal Plains Groundwater Model: Transient Model Set-up and Calibration Report.' Resources and Environmental Management, Adelaide, South Australia.

- Shepherd RG (1975) 'Northern Adelaide Plains groundwater study, Stage II, 1968-74.' Department of Mines South Australia, Report Book 75/38.
- Smith DL (1979) 'Land use and groundwater history of the Northern Adelaide Plains.' Engineering and Water Supply Department, Adelaide, South Australia.
- Teoh K (2006) 'Assessment of Surface Water Resources of Patawalonga Catchment and the Impact of Farm Dam Development.' Department of Water, Land and Biodiversity Conservation, DWLBC Report 2007/09, Adelaide, South Australia.
- Winter TC, Harvey JW, Franke OL, Alley WM (1998) Ground water and surface water - A single resource. In. (U.S. Geological Survey: Denver, Colorado)
- Zulfic D, Osei-Bonsu K, Barnett SR (2008) 'Adelaide Metropolitan Area Groundwater Modelling Project. Volume 1 - Review of Hydrogeology, and Volume 2 - Numerical model development and prediction run.' Department of Water, Land and Biodiversity Conservation, DWLBC Report 2008/05, South Australia.
- Zulfic H (2002) 'Northern Adelaide Plains Prescribed Wells Area Groundwater Monitoring Status Report 2002.' Department of Water, Land and Biodiversity Conservation, DWLBC Report 2002/14, Adelaide, South Australia.



**Government
of South Australia**

Department of Environment,
Water and Natural Resources



**THE UNIVERSITY
of ADELAIDE**



**University of
South Australia**



**Flinders
UNIVERSITY**
ADELAIDE • AUSTRALIA

The Goyder Institute for Water Research is a partnership between the South Australian Government through the Department of Environment, Water and Natural Resources, CSIRO, Flinders University, the University of Adelaide and the University of South Australia.